Spring 5-17-2010

A Microfabrication Approach to Multicellular Mechanics

Zhijun Liu
University of Pennsylvania, liuz@seas.upenn.edu

A Microfabrication Approach to Multicellular Mechanics

Abstract
To address the question of how cell-generated forces regulate the organization and function of endothelial cells, I investigated the mechanical forces in a simple model of cell-cell contact: paired cells contacting each other via a single cell-cell junction. To study the responsiveness of AJs to force, I adapted a system of microfabricated force sensors to quantitatively report both the cell-cell tugging force and the size of adherens junctions (AJ). I observed that AJ size was modulated by tugging force: AJs and tugging force grew or decayed with myosin activation or inhibition, respectively. This myosin-dependent regulation operated in concert with a Rac1, force-independent control of AJ size, and was illustrated by showing that effects of vascular permeability agents (S1P, thrombin) on junctional stability are reversed by changing the extent to which these agents coupled to the Rac and myosin-dependent pathways. Furthermore, I showed that direct application of mechanical tugging force, rather than myosin activity per se, is sufficient to trigger AJ growth.

Inspired by the study of mechanical force on the junctions between two cells, I further extended our tools to measure mechanical force in a more complicated multicellular system involving more cells and more than one type of cells. I investigated the role of mechanical force in a model system of monocytes transmigrating across an endothelial monolayer. Using our force measurement system, I first found that the average traction force in the whole endothelial monolayer increased during monocyte firm adhesion and transmigration. By specifically look at traction forces at the cellular level, I found that the endothelial cell with the monocyte firmly adhered on it showed a much larger traction forces, with the direction of the traction force aligned more centripetally toward the monocyte. Moreover, the sub-cellular and pan-cellular analysis of the traction forces in the monolayer revealed an increase of traction force in local zones vicinity to the monocyte. Finally, engagement of endothelial adhesion molecules could increase traction forces in the endothelial cells. Taken together, this study implicates mechanical forces in firm adhesion and transmigration.

Degree Type
Dissertation

Degree Name
Doctor of Philosophy (PhD)

Graduate Group
Bioengineering

First Advisor
Christopher Chen

Keywords
microfabrication, mechanical force, myosin, endothelial cells

Subject Categories
Biomechanical Engineering | Biomedical Engineering and Bioengineering | Cell Biology

A MICROFABRICATION APPROACH TO MULTICELLULAR MECHANICS

Zhijun Liu

A DISSERTATION

In

Bioengineering

Presented to the Faculties of the University of Pennsylvania

in Partial Fulfillment of the Requirements for the Degree of Doctor of Philosophy

2010

Supervisor of Dissertation

_____
Christopher S. Chen, MD, PhD, Professor

Graduate Group Chairperson

_____
Susan Margulies, PhD, Professor

Dissertation Committee
Prof. Peter F. Davies, PhD
Prof. Peter L. Jones, PhD
Prof. Casim Sarkar, PhD

ACKNOWLEDGEMENT

First, I would like to thank my advisor, Dr. Christopher Chen. I could not imagine a more supportive and fostering advisor, or a more inspiring mentor. I would also like to thank my committee members Drs. Peter Davies, Peter Jones, and Casim Sarkar, for insightful comments, questions, and feedback.

Thanks to my lab members, past and present, for all scientific help and daily moral support; with special thanks to Dan, Colette, Mike, and Ravi, with whom I've had countless conversations throughout my research and life in lab. I would also like to thank my friends, for their unyielding support.

Finally, I would like to thank my parents for giving me the boundless opportunity to pursue a future in science and engineering. Without their hardships and sacrifices, I would not be here and I would not be who I am today.

ABSTRACT

A MICROFABRICATION APPROACH TO MULTICELLULAR MECHANICS

Zhijun Liu

Supervisor: Christopher S. Chen, M.D., Ph.D.

To address the question of how cell-generated forces regulate the organization and function of endothelial cells, I investigated the mechanical forces in a simple model of cell-cell contact: paired cells contacting each other via a single cell-cell junction. To study the responsiveness of AJs to force, I adapted a system of microfabricated force sensors to quantitatively report both the cell-cell tugging force and the size of adherens junctions (AJ). I observed that AJ size was modulated by tugging force: AJs and tugging force grew or decayed with myosin activation or inhibition, respectively. This myosin-dependent regulation operated in concert with a Rac1, force-independent control of AJ size, and was illustrated by showing that effects of vascular permeability agents (S1P, thrombin) on junctional stability are reversed by changing the extent to which these agents coupled to the Rac and myosin-dependent pathways. Furthermore, I showed that direct application of mechanical tugging force, rather than myosin activity per se, is

sufficient to trigger AJ growth.

Inspired by the study of mechanical force on the junctions between two cells, I further extended our tools to measure mechanical force in a more complicated multicellular system involving more cells and more than one type of cells. I investigated the role of mechanical force in a model system of monocytes transmigrating across an endothelial monolayer. Using our force measurement system, I first found that the average traction force in the whole endothelial monolayer increased during monocyte firm adhesion and transmigration. By specifically look at traction forces at the cellular level, I found that the endothelial cell with the monocyte firmly adhered on it showed a much larger traction forces, with the direction of the traction force aligned more centripetally toward the monocyte. Moreover, the sub-cellular and pan-cellular analysis of the traction forces in the monolayer revealed an increase of traction force in local zones vicinity to the monocyte. Finally, engagement of endothelial adhesion molecules could increase traction forces in the endothelial cells. Taken together, this study implicates mechanical forces in firm adhesion and transmigration.

TABLE OF CONTENTS

LIST OF FIGURES

CHAPTER I: INTRODUCTION

Assembly and disassembly of adhesions linking cells to their underlying extracellular matrix and to neighboring cells dictate the organization and re-organization of cells within tissues, and play an essential role in the nearly all multicellular processes ranging from tissue morphogenesis to cancer metastasis to the control of barrier properties in cellular sheets (Dejana, Corada et al. 1995; Cavallaro and Christofori 2004; Gumbiner 2005). Regulating the strength of such adhesions through changes in the distribution and expression levels of various adhesion receptors, including integrins and cadherins, appears to precede and drive the movement and reorganization of cells during numerous developmental processes such as tubulogenesis, compaction, convergent extension, and epithelial-mesenchymal transition (Gumbiner 2005). Experimentally varying the degree of cell-cell cohesivity and cell-substratum adhesivity in culture leads to predictable changes in how two types of tissue will sort, spread over each other, and self-assemble based on the differential adhesion hypothesis (Steinberg 1970; Foty, Pfleger et al. 1996).

In addition to receptor-mediated mechanisms, recent findings suggest that mechanical forces can drive changes in multicellular organization through altering the architecture of cell-cell adhesions. During gastrulation, activation of myosin II triggers apical constriction in cells of the ventral furrow, causing these cells to invaginate (Dawes-Hoang, Parmar et al. 2005; Martin, Kaschube et al. 2009). Myosin II also drives the stereotypical redistribution of cell-cell contacts that accompany tissue extension by cell

intercalation (Bertet, Sulak et al. 2004; Rauzi, Verant et al. 2008; Skoglund, Rolo et al. 2008; Rolo, Skoglund et al. 2009). Loss of myosin heavy chain IIA impairs cell-cell adhesion in embryoid bodies (Conti, Even-Ram et al. 2004). **Such studies have suggested a role for mechanical force in regulating cell-cell junctions.**

The endothelial cell monolayer controls the passage of molecules and leukocytes into and out of the bloodstream. Such dynamic barrier function plays a critical role in tissue maintenance and repair, angiogenesis, and inflammation. During both innate and adaptive immune responses, the trans-endothelial migration (TEM, also known as extravasation or diapedesis) of leukocytes across the endothelial barrier is a tightly controlled process involving multiple steps. While we already have a plenty of knowledge of the molecular and cellular signals involved in rolling, adhesion, and even transmigration (Petri and Bixel 2006; Vestweber 2007), we are just starting to unveil the mechanical signals in this process and their coordination with molecular signals. Previous studies have focused on the mechanical force in leukocytes, but **the changes of mechanical force in endothelial cells, especially after firm adhesion, has never been directly measured and characterized.**

1.1 Cell-cell Adhesions

Adherens junctions (AJs) formed through the homotypic binding between cadherins are one of many types of junctions that assemble at sites of cell-cell contact, and appear to be important for regulating the strength of cell-cell adhesion (Leckband and Prakasam 2006). The highly conserved, ~150 amino acid cytoplasmic domain of cadherins binds to β-catenin /plakoglobin and α-catenin, which in turn mediates the anchorage of the cadherin- β-catenin complex to the actin cytoskeleton, either directly or through numerous intermediate scaffolding proteins like vinculin, α-catenin, ZO-1 and ZO-2 (Pokutta and Weis 2002). They require the activity of the Rho GTPases Cdc42, Rac and RhoA for the clustering of cadherins, in addition to the subsequent assembly AJs (Braga, Machesky et al. 1997; Takaishi, Sasaki et al. 1997; Wojciak-Stothard and Ridley 2002). These physical and regulatory links to the actin cytoskeleton appear to provide AJs with the ability to physically anchor cells to the neighboring cells, and to withstand substantial forces (Chen, Tan et al. 2004). AJs are similar in architecture, share common components, and undergo cross talk with FAs—the adhesive junctions to the matrix (Pokutta and Weis 2002; Chen, Tan et al. 2004). The similarities between FAs and AJs also foreshadow a role for mechanical forces in regulating AJs.

1.2 The Force Generating Apparatus in Cells

Cells exert nanonewton-scale contractile forces against adhesive structures that couple the cell to its external environment. Inside cells, mechanical forces are generated by stress fibers formed by the bundling of actin and myosin molecules, and connected to focal adhesions and adherence junctions to physically transmit the force to the external environment and the neighboring cells (Burridge, Fath et al. 1988; Katoh, Kano et al. 1998). In the molecular level, contractile forces are generated by the cross-bridging and rowing activity of myosin molecules anchored along the filamentous-actin fibers, energized by the hydrolysis of ATP (Huxley 1969; Rayment, Holden et al. 1993). The major non-muscle myosin, myosin II, contains two heavy chains constituting the head and tail domains, and four light chains binding the heavy chains in the "neck" region between the head and tail (Somlyo and Somlyo 2003). The regulation of myosin (IIA, IIB, and IIC) depends on the reversible phosphorylation of the regulatory light chain on Ser 19, which is phosphorylated by more than a dozen kinases including myosin light chain kinase (MLCK; also known as MYLK), Rho-associated, coiled coil-containing kinase (ROCK), myotonic dystrophy kinase-related CDC42-binding kinase (MRCK; also known as CDC42BP) and etc (Vicente-Manzanares, Ma et al. 2009). Myosin II filament assembly is regulated by phosphorylation of the myosin II heavy chain (NMHC II) coiled-coil and tail domains (Vicente-Manzanares, Ma et al. 2009).

1.3. The Relationship between Mechanical Force and Cell-cell Adhesions

Actomyosin contractility affects cellular organization within tissues, in part through the generation of mechanical forces at sites of cell-matrix and cell-cell contact (Burridge and Chrzanowska-Wodnicka 1996; Mege, Gavard et al. 2006; Schwartz and DeSimone 2008). While increased mechanical loading at cell-matrix adhesions results in cytoskeletal reinforcement (Choquet, Felsenfeld et al. 1997; Galbraith, Yamada et al. 2002) and focal adhesion growth (Riveline, Zamir et al. 2001; Sniadecki, Anguelouch et al. 2007), the role of mechanical force in regulating cell-cell adhesion remains to be determined. Another physiological model system for exploring the relationship between mechanical forces and the organization of junctional proteins is endothelial barrier function, in which physiological signals regulate junctions to control vascular permeability through a mechanism that requires acto-myosin contractility. The increase in vascular permeability by inflammatory agents such as thrombin is associated with disruption of cell-cell contacts through increased RhoA-mediated myosin-generated contraction (van Nieuw Amerongen, Draijer et al. 1998; Dudek and Garcia 2001). Paradoxically, RhoA, myosins, and local actin polymerization have also been associated with clustering of cadherins and assembly of adherens junctions (AJs) (Adams, Nelson et al. 1996; Braga, Machesky et al. 1997; Vasioukhin, Bauer et al. 2000; Shewan, Maddugoda et al. 2005; Yamada, Pokutta et al. 2005). These findings suggest that myosin signaling might lead to opposing effects. An intriguing possibility is that activated myosin, depending on different stimulation contexts, might lead to

fundamentally different resultant forces produced at cell-cell adhesions. This highlights the need to directly measure forces at cell-cell adhesions, as a path toward constructing a paradigm by which local forces regulate intercellular adhesion

1.4 Current Techniques to Measure Cell-cell Forces

Various systems have been developed to exert local forces onto cell-cell adhesions using atomic force microscopy (AFM), pipettes, or magnetically trapped beads (Potard, Butler et al. 1997; Baumgartner, Hinterdorfer et al. 2000; Ko, Arora et al. 2001; Chu, Thomas et al. 2004; Perret, Leung et al. 2004; Panorchan, Thompson et al. 2006) . Pulling or twisting of beads bound to cadherins with ~30-150 pN forces are sufficient to elicit cellular signaling and actin assembly (Potard, Butler et al. 1997; Ko, Arora et al. 2001). However, three orders of magnitude greater force (~200 nN) are required to break cell-cell adhesion between suspended cells expressing E-cadherin (Chu, Thomas et al. 2004). While these studies begin to describe the sensitivity and ultimate strength of the junction, and have provided a wide range of forces which cells can experience at cell-cell adhesions, these studies fail to capture endogenous forces experienced at the junction and whether these forces change in different physiologic settings.

CHAPTER II: MECHANICAL FORCE REGULATES THE SIZE OF CELL-CELL JUNCTIONS

2.1 Background

Cell-generated contractile forces drive changes in multicellular organization through numerous mechanisms, including altering the architecture of cell-cell contacts. During gastrulation, activation of myosin II triggers apical constriction in cells of the ventral furrow, causing these cells to invaginate (Dawes-Hoang, Parmar et al. 2005; Martin, Kaschube et al. 2009). Myosin II also drives the stereotypical redistribution of cell-cell contacts that accompany tissue extension by cell intercalation (Bertet, Sulak et al. 2004; Rauzi, Verant et al. 2008; Skoglund, Rolo et al. 2008; Rolo, Skoglund et al. 2009). Loss of myosin heavy chain IIA impairs cell-cell adhesion in embryoid bodies (Conti, Even-Ram et al. 2004). Such studies have suggested a role for myosin in regulating cell-cell junctions.

Adherens junctions (AJ), in particular, appear sensitive to mechanical regulation. Inhibition of Rho kinase, MLCK, myosin ATPase activity or expression interferes with the growth and maintenance of adherens junctions in several experimental systems (de Rooij, Kerstens et al. 2005; Shewan, Maddugoda et al. 2005; Miyake, Inoue et al. 2006; Ivanov, Bachar et al. 2007; Yamada and Nelson 2007; Abraham, Yeo et al. 2009). E- and N-cadherin cluster in a myosin-dependent fashion, forming focal adhesion-like structures when cells are plated on substrates coated uniformly with cadherin extracellular domains (Delanoe-Ayari, Al Kurdi et al. 2004; Gavard, Lambert et al. 2004; Shewan, Maddugoda et al. 2005; Lambert, Thoumine et al. 2007). While these findings suggest that myosin activity is required for junction assembly, the functional importance of mechanical forces

experienced at cell-cell contacts per se remains unknown, since such forces have not been measured.

Herein, we describe a method to measure the intercellular tugging forces that neighboring cells exert on each other across their cell-cell adhesions, using a microfabricated force-sensor device. We find that endothelial cells generate substantial forces that pull normal to the face of the cell-cell contact, designated as the intercellular *tugging force*. We reveal that the AJ size is regulated by tugging force, and the growth of AJs in response to increased tugging force follows a simple first order relationship. Importantly, we observe that cell-cell tugging force cooperates with a Rac-mediated force independent pathway to determine the ultimate size of AJs. Uncoupling these two pathways, as occurring when cells are stimulated with thrombin, triggers force-dependent disruption of cell-cell adhesions. These findings demonstrate that coupling the actomyosin-generated mechanical stresses at focal adhesions (traction stresses) to cell-cell contacts (intercellular tugging stresses) provides a means to dynamically reorganize cell-matrix and cell-cell adhesions locally, and suggests that cell-generated forces can influence the architecture of tissues by regulating the strength of cell-cell adhesions.

2.2 Materials and Methods

2.2.1 Preparation of Substrates

Elastomeric microneedle array substrates were fabricated via polydimethylsiloxane (PDMS; Sylgard 184, Dow-Corning, Midland, MI)-based replica-molding and patterned with fibronectin by micro-contact printing as described previously(Tan, Tien et al. 2003). The fibronectin patterns consist of bowtie-shaped regions each with a total area of 1600 μm2 and coverage of ~30 microneedles. Subsequently, microneedles were fluorescently labeled with 5 μg/ml Δ^9-DiI (1,1'-dioleyl-3,3,3',3'- tetramethylindocarbocyanine methanesulfonate; Invitrogen, Carlsbad, CA). Cell adhesion was restricted to the bowties by blocking the unprinted surface with 0.1% Pluronics F127 (BASF, Mount Olive, NJ). Glass coverslips that had been coated with a thin layer of PDMS were similarly patterned with bowtie-shaped fibronectin islands. Bare glass coverslips were uniformly coated with fibronectin by adsorbing 5 μg/ml fibronectin (BD Biosciences, San Jose, CA) for 1 hour.

2.2.2 Cell Culture

Bovine adrenal microvascular endothelial cells (BAMECs, VEC Technologies, Rensselaer, NY) were cultured in 10% fetal bovine serum (Hyclone, Logan, UT), 10 ng/ml EGF, 3 ng/ml bFGF, and antibiotics in low glucose DMEM. Human pulmonary artery endothelial cells (HPAECs, Lonza, Basel, Switzerland) were cultured in EGM-2 complete medium (Lonza) supplemented with 10% fetal bovine serum (Sigma, St. Louis, MO). Cells were seeded onto substrates in normal serum-containing media and allowed to spread overnight before fixation or further treatment. For monolayer experiments, HPAECs were grown to confluence over 1-2 days on glass coverslips prior to fixation or additional treatment.

2.2.3 Reagents

Recombinant adenovirus encoding human vascular endothelial (VE)-cadherin lacking the β-catenin binding domain (VE-Δ) was prepared using the AdEasy XL system (Stratagene, La Jolla, CA) as previously described (Nelson, Pirone et al. 2004). Recombinant adenoviruses encoding RacV12 and GFP-tagged VE-cadherin were generous gifts of Drs. Anne Ridley and Sunil Shaw, respectively. To induce expression of VE-Δ or RacV12, HPAECs were infected with virus for 6 hours prior to seeding onto substrates. To express GFP-tagged VE-cadherin, HPAECs were infected with virus for 5 days prior to seeding onto substrates (see Live-cell imaging section). siRNA duplexes for myosin IIA, IIB, and cyclophilin were purchased from MWG Operon, based on previously validated sequences(Ivanov, Bachar et al. 2007). HPAECs were transfected with siRNA duplexes (100 nM) using Lipofectamine RNAiMAX (Invitrogen, Carlsbad, CA). For experiments involving thrombin or S1P, cells were starved in 1% serum for 8~10 hours, and then stimulated with thrombin (0.1 μM, 10 units/ml, Enzyme Research Lab, South Bend, IN) or S1P (1 μM, Sigma, St. Louis, MO) for 10 minutes prior to fixation. To disrupt cytoskeletal tension, cells were exposed to blebbistatin (30 μM, Tocris, Ellisville, MO) for 2 hours, or Y-27632 (25 μM, EMD Biosciences, San Diego, CA) for 1 hour. To increase cytoskeletal tension, cells were treated with nocodazole (1 μM, Sigma, St. Louis, MO) for 10 minutes, Calyculin-A (1 nM, Cell Signaling Technology, Danvers, MA) for 10 minutes, or RhoA-Q63L (see Live-cell imaging section; Cytoskeleton, Denver, CO). For inhibition of Rac1, cells were treated with NSC23766 (10 μM, Calbiochem, San Diego, CA) for 1 hour.

2.2.4 Generation of Lentiviral Myosin Light Chain

The cDNA encoding human myosin light chain 2 (MGC clone 3505) was purchased from ATCC (Manassas, VA). This cDNA was subcloned into the lentiviral plasmid, pRRL, using 5' EcoRI and 3' XhoI sites. Subsequently, an IRES-GFP cassette was added 3' to the MLC2 cDNA (5' XhoI and 3' NheI sites). The phosphomimetic mutations (T18D, S19D) were introduced using Quikchange mutagenesis kit (Stratagene, La Jolla, CA). PCR oligos were as follows, with mutated nucleotides capitalized: 5'aagcggccacagcgggccGATGAcaatgtcttcgcaatgtttgac3' (sense) and 5'gtcaaacattgcgaagacattgTCATCggcccgctgtggccgctt3' (antisense). Lentivirus was prepared in 293x cells using the Lenti-X system (Clontech, Mountain View, CA). HPAEC infections were done with a spinfection protocol, 1200g for 90 minutes. Viruses were titered based on GFP expression.

2.2.5 Measurement of Tugging Forces

To measure the bending of the microneedles, fluorescent images of the tips and base of the DiI-labeled microneedles were acquired by confocal microscopy (Ultraview, Perkin Elmer, Wellesley, MA). The centroids of the microneedles at both the tip and base were determined by localized thresholding using an automated Matlab program (Lemmon, Sniadecki et al. 2005) (Mathworks, Natick, MA), to yield the deflected and undeflected positions, respectively. The tip and base centroids are then aligned by minimizing the difference in the centroid coordinates of microneedles not attached to cells, or free microneedles. To calculate the force on each microneedle, the difference between the tip and base centroids is multiplied by the spring constant of the microneedle (32 nN/μm). The uncertainty in the measurement of microneedle deflection is ~0.1 μm, as assessed by the standard deviation of the deflections of free microneedles. As such, the uncertainty in force measurement is ~3.2 nN. Within a bowtie of two cells, AJ staining was used to identify which microneedles were attached to each cell, and the force vectors on the two subsets of microneedles were summed to calculate the tugging force experienced by each cell.

2.2.6 Immunofluorescence Imaging and Analysis

Cells were fixed in 4% paraformaldehyde, blocked in goat serum, incubated with antibody against β-catenin (BD Biosciences, San Jose, CA) and then detected with fluorophore-conjugated isotype-specific anti-IgG antibodies (Invitrogen, Carlsbad, CA). Fluorescence images were acquired on a Zeiss Axiovert 200M (Zeiss MicroImaging, Thornwood, NY) and processed in Matlab to quantify junctional area. AJ staining was binarized (for both pairs of cells on microneedles and monolayers) by thresholding to eliminate the dimmest pixels (25% and 10%, respectively). This approach for AJ quantification was validated using confocal microscopy. Measurement of AJ size in epi-fluorescence gave comparable results to a more rigorous volume-metric analysis (see Fig. 1). For monolayers, a single layer erosion filter also was applied to remove speckles with diameters of less than two pixels. It should be noted that in endothelial cells, area is a reasonable estimate of the size of AJs given that electron microscopy analyses show that the endothelial cell-cell interface forms obliquely, nearly co-planar with the underlying matrix (Dejana 2004).

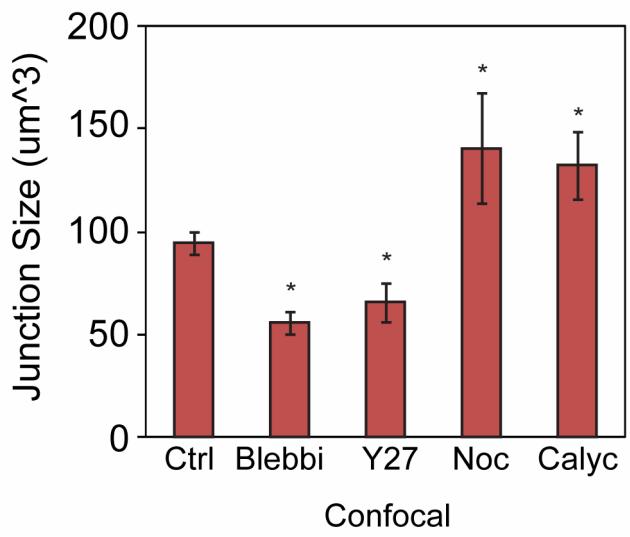

Figure 1. Confocal volume analysis of adherens junction size

Confocal imaging of bowties was done using a Zeiss LSM-510 Meta confocal microscope (Penn Biomedical Imaging Core). AJs were visualized by β-catenin staining and the volumes of AJs were analyzed with Zeiss LSM image analysis software. Bar graphs showing average junction size (volume) in bowtie pairs exposed to vehicle control (Ctrl), blebbistatin (30 μM, Blebbi), Y27632 (25 μM, Y27), nocodazole (1μM, Noc) calyculin-A (1nM, Calyc). * $p < 0.05$, indicates comparison against vehicle control. Error bars on all graphs denote standard error of the mean.

2.2.7 Live-cell Imaging

HPAECs expressing GFP-tagged VE-cadherin were seeded onto bowtie-patterned substrates (either microneedle substrates or PDMS-coated coverglass) and imaged with a 60x objective on a Nikon TE2000 (Nikon Instruments Inc., Melville, NY) equipped with a temperature and CO_2-controlled cage incubator. Fluorescence images at 488 nm (GFP) and 594 nm (DiI-labeled microneedles), and phase images were collected at one-minute intervals. Bowties were monitored for at least 10 minutes after which one cell in the bowtie pair was either injected with constitutively active RhoA Q63L, or mechanically pulled by bringing a rigid fibronectin-coated microcapillary tip into contact with the cell and dragging the tip away from the junction. Cell-cell junctions were imaged for an additional 30 minutes following microinjection or pulling. Measurements of live-cell traction and tugging forces on microneedle substrates were performed as described for fixed samples (see Methods). AJ size in microinjected/micropulled bowties on flat PDMS were measured by quantitative image analysis of the GFP-VE-cadherin. Fluorescence images were processed using built-in functions in IPLab software (BD Biosciences, Rockville, MD), namely a background subtraction, followed by a medium blur function to remove pixelation. Matlab was then used to determine AJ size from the processed images.

2.2.8 RhoA and Rac1 Activity Assay

RhoA and Rac1 activity were assayed using the RhoG-LISA and RacG-LISA kits, respectively (Cytoskeleton). Briefly, HPAECs were grown to confluence in 60mm dishes, and starved overnight in medium containing 0.5% FBS. Thrombin (0.1 μM) and S1P (1μM) were added to the HPAECs monolayers for 1 minute, followed by cell lysis, and Rho GTPase activity measurement as per the manufacturer's protocol.

2.2.9 Statistical Analysis

Data are expressed as mean ± s.e.m. or mean ± s.d. as indicated in the figure legends. Linear regression and Student's t-test were performed for statistical analysis. For ellipse-fitting, data was fit with the least-squares ellipse using Matlab (Halir and Flusser 1998). The trend band of junction size at different tugging force levels is plotted as a moving average (darker gray line) ± 99% Confidence Interval (CI, lighter gray region) using built-in Matlab functions.

2.3 Results

2.3.1 An Approach to Measure Tugging Forces

Here we describe a system to quantify the tugging force applied to cell-cell junctions, and investigate how such tugging forces affect the AJ. To measure tugging force, we retooled a previously described approach which reports traction forces based on deflections within an array of elastomeric microneedles (Tan, Tien et al. 2003) (Fig. 2A-C, Equation 1). Cells exist in quasi-static equilibrium where net force sums to zero (Balaban, Schwarz et al. 2001; Tan, Tien et al. 2003) (n.b., an imbalance of 1 nN would accelerate a 10ng cell at 100 m/s^2). For a cell in contact with a neighbor, the net force encompasses both traction forces and the intercellular tugging force experienced at the cell-cell contact (Fig. 2D-F). Since the net force remains zero, the intercellular tugging force, F_c, is equal in magnitude and opposite in direction to the measured net traction force reported by the microneedle array (Fig. 2F; Equation 2). A key feature of this system is the formation of a single well-defined contact between two neighboring cells; calculating forces across multiple cell-cell contacts becomes mathematically insoluble. Because random seeding yields few cells that form only a single cell-cell contact, we enhanced pair formation by patterning fibronectin into bowtie-shaped regions (Tan, Tien et al. 2003)(Fig. 2G,H).

To determine whether cells exert a measurable intercellular F_c, we assayed forces in endothelial cells seeded as singlet or in contacting pairs on the microneedle substrates

(Fig. 2A, B). In contacting cells, but not singlets, we observed a substantial F_c (~40 nN), that was oriented roughly normal to the face of the AJ and was sustained over several hours (Fig. 2J,K). No difference in average traction force per microneedle was observed between singlet and contacting cells (Fig. 2L).

To confirm that the observed F_c reflects contractile forces transmitted to the AJ, we tested whether decoupling VE-cadherin from the actin cytoskeleton perturbed F_c. Expression of a cadherin mutant with a truncated cytoplasmic tail (Navarro, Caveda et al. 1995) decreased F_c to nearly half the level measured in GFP expressing control cells (Fig. 2M-O), whereas traction forces remained similar (Fig. 2P). Thus, tugging forces are applied to the AJ through coupling of VE-cadherin to the actin cytoskeleton.

AJ size (indicated by β-catenin staining) was heterogeneous in the bowtie patterns (Fig. 2Q,R). Quantitative comparison revealed a linear correlation between the size of AJs and the magnitude of F_c, resulting in an apparent constant stress of ~1 nN/μm^2 (Fig. 2S). In contrast, AJ size and traction force per microneedle were uncorrelated (Fig. 2T). Thus the correlation between AJ size and force appears to be specific to changes in local *tugging* force rather than global cellular contractility.

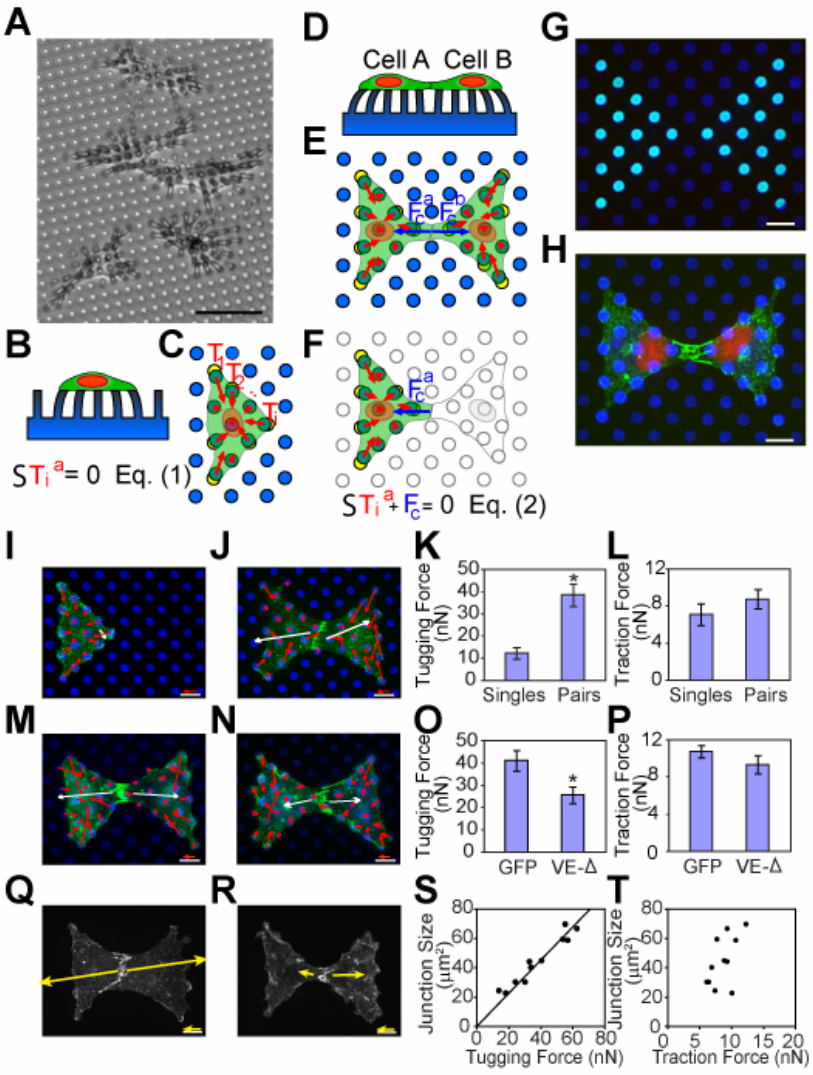

Figure 2. An approach to measure tugging forces

(**A**) Endothelial cells exert contractile forces that strongly deflect underlying microneedles (phase contrast image; scale bar, 50 μm).

(**B-C**) The vector sum of individual traction forces, T_n, (red arrows) exerted by a cell is zero (Fig. 2B, C, Equation 1) as cells are in quasi-static equilibrium (Balaban, Schwarz et al. 2001; Tan, Tien et al. 2003)

(**D-E**) For a pair of contacting cells, the net force encompasses both traction forces (red arrows) and the intercellular tugging force, F_c, (blue arrows).

(**F**) The intercellular tugging force is equal in magnitude and opposite in direction to the measured net traction force reported on the microneedle array (Equation 2). We define the vector convention for F_c as follows: F_c plotted over cell A is the net tugging force that cell A is exerting on cell B at the cell-cell contact. Cell B is expected to pull on cell A with an equal and opposite force.

(**G-H**) Cells were constrained to a bowtie pattern using microcontact printing of fibronectin. Immunofluorescence showing patterned fibronectin in cyan (**G**) and formation of adherens junctions in green (anti-β-catenin, **H**). Microneedles and cell nuclei were counterstained with DiI (blue) and DAPI (red), respectively. Scale bar, 10 μm.

(**I, J**) Representative force vector plots of single (**I**) and paired (**J**) cells. Force vectors are plotted as arrows showing the direction of force and magnitude (reflected by arrow length; reference arrows for 10nN force shown above scale bar). Individual traction forces are shown in red and tugging force is shown in white. Small, force imbalances are observed due to uncertainties in microneedle deflection measurements. The error in the vector sum of individual traction forces equals the error of the individual forces multiplied by the square root of the number of tractions. The microneedles typically have an error of +/-3 nN, and cells span on average 15 microneedles, leading to an expected

noise level of 12 nN in the determination of F_c. Tugging forces occurred roughly normal to the contact, with less than 20 degrees deviation from the longitudinal axis of the bowtie, in 22 out of 28 measured bowtie pairs.

(**K**) Average F_c experienced in bowtie pairs of HPAECs. * $p < 0.05$, indicates comparison against single cells.

(**L**) Average traction force per microneedle was similar in singlet or contacting cells.

(**M-O**) Tugging forces require coupling between VE-cadherin and the actin cytoskeleton. Cells expressing adeno-VE-Δ, a truncated VE-cadherin mutant lacking the β-catenin binding domain, form adherens junctions (anti-β-catenin, green, **N**) but show greatly diminished tugging force compared to adeno-GFP infected cells (**M**, **O**). * $p < 0.05$, indicates comparison against GFP.

(**P**) Average traction force per microneedle was unaffected by VE-Δ expression.

(**Q, R**) AJ (anti-β-catenin) in HPAECs are heterogeneous in size. Tugging force is shown in yellow.

(**S**) AJ size is linearly correlated with F_c, with a correlation coefficient $R^2 \approx 0.9$. Each data point represents one pair of cells.

(**T**) AJ size is not correlated with with the average traction force per microneedle.

Error bars on all graphs denote standard error of the mean.

2.3.2 Tugging Force Regulates the Size of Adherens Junctions.

These data suggested the possibility that cell-cell junction assembly, much like focal adhesion assembly, is a force-dependent process. To test this hypothesis, we antagonized cytoskeletal tension by treatment with Y-27632 (a Rho kinase inhibitor) or blebbistatin (myosin II ATPase inhibitor). Both inhibitors substantially decreased average traction force and F_c, and caused a reduction in AJ size, preserving the linear relationship between F_c and junctions (Fig. 3A-D). Likewise, siRNA-mediated knockdown of either myosin IIA or IIB decreased traction force, F_c, and junction size (Fig. 3A-C,E).

These data are consistent with a reported requirement for myosin in maintaining adherens junctions (Conti, Even-Ram et al. 2004; Shewan, Maddugoda et al. 2005; Miyake, Inoue et al. 2006; Ivanov, Bachar et al. 2007; Yamada and Nelson 2007; Abraham, Yeo et al. 2009). However, whether *increasing* myosin-mediated tension *promotes* AJ assembly is largely untested. We therefore assayed the effects of the tension-inducing drugs, nocodazole, and calyculin-A, in our system. Both agents significantly increased traction force, F_c, and AJ assembly (Fig. 3B,C,F), supporting a role for tension-induced AJ assembly, but they lack molecular specificity for targeting myosin. To address this limitation, we infected cells with lentivirus encoding phosphomimetic mutants (T18D, S19D) of myosin regulatory light chain (MLC) to test

directly the effect of myosin activation. Phosphomimetic MLC, but not wild-type MLC, dramatically enhanced average traction force and F_c, and induced more expansive AJs (Fig. 3B,C,G).

Remarkably, compiling all of our studies with tension manipulations revealed a general relationship between AJ size and F_c that spanned a wide range of AJ areas (~7-87 μm^2) and F_c (~7-120nN) (Fig. 3H). Using moving average and bootstrap methods to calculate the mean and 99% percent confidence interval, one can appreciate a linear relationship between AJs and F_c in the smaller force/AJ regime, whereas the response of AJ begins to saturate at forces higher than ~70nN, suggesting an upper limit for mechanosensitive growth of AJs.

To examine whether this force-AJ relationship can be generalized, we characterized the response of AJs in conventional monolayers to tension manipulations. Consistent with the bowtie system, treatment of monolayers with tension antagonists reduced AJ levels as compared to unstimulated cells (Fig. 3I-K). Conversely, upregulation of tension increased the size of AJs in the monolayers (Fig. 3I,J,L). Thus, tugging forces appear to regulate junction size, regardless of experimental culture conditions (bowties versus monolayers).

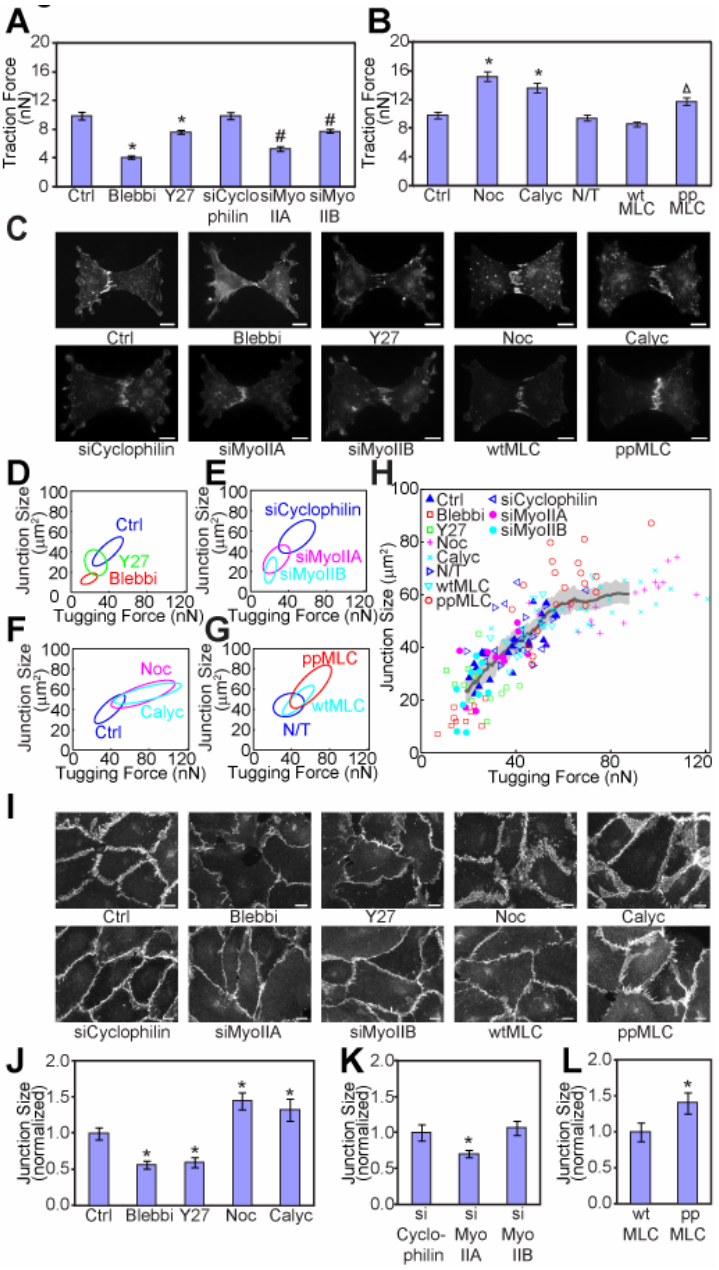

Figure 3. Tugging force regulates the size of adherens junctions

(**A, B**) Tension antagonists and agonists modulate average traction force per microneedle and F_C. The following antagonists were used: blebbistatin (30 μM, Blebbi), Y27632 (25

μM, Y27), siRNA against myosin IIA (siMyoIIA), myosin IIB (siMyoIIB). Tension agonists included nocodazole (1μM, Noc) calyculin-A (1nM, Calyc), lentivirally encoding phosphomimetic light chain (ppMLC). Control conditions included vehicle control (Ctrl), control siRNA (siCyclophilin), no treatment (N/T), or lentiviral wild-type MLC (wtMLC). * $p < 0.05$, indicates comparison against vehicle control, # $p < 0.05$, indicate comparison against control siRNA, and Δ $p < 0.05$, indicate comparison against wtMLC. (**C**) AJ size is regulated by changes in actomyosin-mediated tension. Bowtie pairs exposed to the tension-manipulating conditions as described in (**A, B**), and stained for β-catenin.

(**D-G**) Relationship between AJ size and manipulations of F_c. Inhibition of F_c by blebbistatin, Y27632 (**D**), or treatment with siRNA against myosin II A or B (**E**) leads to reduced junction size, whereas elevated F_c following stimulation with nocodazole, calyculin-A (**F**), or infected with lentivirus encoding phosphomimetic mutants (**G**) increased junction size. AJ size and F_c measurements (at least 10 bowtie pairs per condition) were clustered and plotted as an elliptical fit (**D-G**).

(**H**) A scatter plot showing the correlation between AJ size and F_c across all conditions. Trend line was determined using a moving average method (dark gray line; light gray band shows ± 99% Confidence Interval).

(**I-L**) Tension manipulations affect AJs in monolayers. Immunofluorescence images

showing changes in AJs (anti- β -catenin) in HPAECs monolayers exposed to tension-manipulating conditions (**I**). Quantification of monolayer junctional response (**J-L**). * $p < 0.05$, indicates comparison against control monolayers: Ctrl (**J**), siCyclophilin (**K**), or wtMLC (**L**).

All scale bars are 10 μm. Error bars denote standard error of the mean.

2.3.3 Modulation of Force-AJ Relationship by Soluble Factors.

While the aforementioned tension manipulations reveal an important linkage between myosin activity, tugging forces, and regulation of AJ size, these treatments lack a physiological context. We hypothesized that physiological stimuli may also control the homeostasis of cell-cell junctions in endothelium through tugging forces. Inflammatory agents such as thrombin have been proposed to disrupt of cell-cell contacts through increased RhoA-mediated myosin-generated contraction (van Nieuw Amerongen, Draijer et al. 1998; Dudek and Garcia 2001), which represents a counter-example to the stimulatory effects of myosin contractility on AJs observed here (Fig. 3). Sphingosine-1-phosphate (S1P), another vasoactive compound, appears to strengthen cell-cell contact (McVerry and Garcia 2004) at a concentration that does not impact cellular contractility (Shikata, Birukov et al. 2003), hinting at the possibility of a force-independent modulation of junction size.

Application of thrombin or S1P to monolayers of HPAECs induced the expected disruption or enhancement of AJ assembly, respectively (Fig. 4A,B). To clarify how these permeability agents impact AJs, we assayed AJs and F_c in the bowtie-microneedle system. Traction force and F_c increased in response to thrombin without a concomitant increase in junction size (Fig. 4C-E), resulting in a precipitous rise in mechanical stress at the junction (from ~1 to ~8 nN/μm^2). In fact, thrombin induced breakage of cell-cell contacts in numerous bowties, and those AJ that were spared were shorter, fainter, and

less distinct relative to controls (Fig. 4B). In contrast, S1P stimulated expansive junctions that took a tortuous path across the cell-cell contact, but had no significant effect on F_C (Fig. 4D,E), and thus reduced junctional stress (to ~0.5 nN/μm^2).

The ability of S1P to enhance junction formation without increasing F_C, and thrombin to induce F_C without increasing junction assembly, implies a mechanism of AJ growth that is independent of F_C, or one that modulates the coupling of AJ growth to F_C. Because Rac1 is implicated in S1P signaling and in AJ assembly (Braga 2002; Shikata, Birukov et al. 2003; Cullere, Shaw et al. 2005; Fukuhara, Sakurai et al. 2005; Mehta, Konstantoulaki et al. 2005; Yamada and Nelson 2007; Baumer, Drenckhahn et al. 2008; Perez, Tamada et al. 2008), we postulated that changes in Rac1 activity might contribute to the observed regulation of AJs. We therefore measured Rac activity, and RhoA activity (an upstream mediator for myosin/tension driven responses), as a function of thrombin or S1P treatment. Thrombin robustly activated RhoA, while *suppressing* Rac activity (Fig. 4F). In contrast, S1P specifically upregulated Rac activity, while leaving RhoA unperturbed (Fig. 4F). These data suggested a direct correlation between junction size and Rac activity. Indeed, inhibition of Rac activity using NSC23766 (10 μM) abolished S1P-induced AJ assembly, and demonstrated a requirement for Rac in regulating junction growth (Fig. 4H,I).

We then tested whether changes in Rho and Rac activity also contributed to thrombin-induced junctional disassembly. Pre-treatment with Y27632 inhibited the thrombin-induced increase in traction forces and F_c, and prevented the disruption of junctions (Fig. 4G-I). Remarkably, expression of a constitutively active Rac mutant (RacV12) prevented thrombin-induced disassembly (Fig. 4G-I). These finding suggest that Rac activity and tugging force are both important determinants in the response of AJs to vasoactive compounds.

To examine whether Rac activity indeed cooperates with F_c to regulate AJ size, we examined the effect of jointly manipulating tension and Rac activity. RacV12 alone induced junction assembly without altering tugging forces, suggesting AJ growth does not require an *increase* in basal F_c. However, treatment of RacV12 cells with blebbistatin partially inhibited AJ assembly, demonstrating that Rac-induced junctions remained dependent on baseline tugging forces (Fig. 4J-L). Conversely, inhibition of Rac with NSC23766 attenuated the ability of phosphomimetic myosin to promote junction growth (Fig 3J,K,M) further evidencing the hypothesis that Rac activity provides a permissive context for force-induced junction growth. Again, similar effects were observed in monolayers as in our bowtie system, suggesting that these relationships between Rho, Rac, and junction assembly are conserved in more general settings (Fig. 4N,O). Together, these studies suggest a model whereby Rho-mediated myosin activity

generates tugging forces, and Rac mediates the ability of AJs to assemble in response to those forces (Fig. 4P).

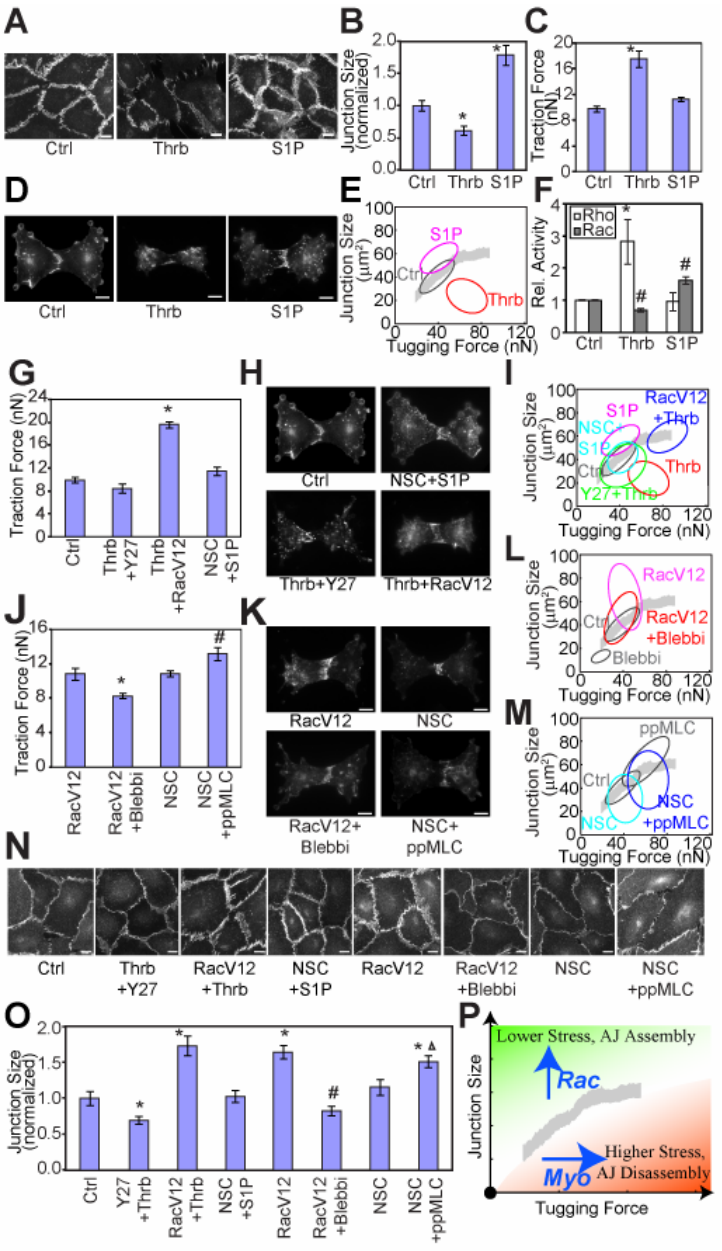

Figure 4. Modulation of force-AJ relationship by soluble factors

(**A-B**). Vasoactive compounds S1P and thrombin coordinately upregulate and downregulate adherens junctions. (**A**) Monolayers exposed to vehicle only (Ctrl), thrombin (0.1 μM, Thrb), or S1P (1μM, S1P) show S1P-induced AJ growth and

thrombin-induced AJ disassembly (anti-β-catenin staining). (**B**) Quantification of changes in AJs in monolayer cultures shown in (**A**). * $p < 0.05$, indicates comparison against control.

(**C**) Thrombin, but not S1P, induces cellular tension. Bar graph showing average traction force per microneedle reported in bowtie pairs stimulated with vasoactive compounds.

(**D-E**) Effects of thrombin and S1P on junctional size-tugging force relationship. S1P and thrombin alter AJ formation (anti-β-catenin) in bowtie pairs (**D**). Relationship between AJ and F_c data plotted as an elliptical fit (**E**). The trend band and control condition from Fig. 3 are re-plotted here for reference.

(**F**) RhoA and Rac1 activity assay for Thrombin and S1P using RhoGliza and RacGliza kits, respectively. Plot shows the range of data across two independent experiments, normalized to the mock-treated control.

(**G**) Manipulations of Rac activity do not alter cellular tension, as assayed by average traction force per microneedle. In contrast, inhibition of Rho kinase (Y27632, 25μM) blocks thrombin-induced tension. * $p < 0.05$, indicates comparison against control.

(**H-I**) Altering the coupling of S1P and thrombin to Rac and tension-dependent pathways reverse the effects of these vasoactive compounds on junctions. S1P-induced AJ growth is inhibited by treatment with NSC23766 (10 μM), whereas thrombin-induced AJ disassembly is blocked by expression of constitutively active Rac (RacV12). AJ junctions visualised by β-catenin localization (**H**). Decoupling thrombin from cellular tension or forcibly linking it to constitutively active Rac restores the linear relationship

between AJ and tugging force. Similarly, inhibiton of Rac1 with NSC23766 restores the normal AJ-tugging force balance in S1P-stimulated cells.

(**J**) Myosin-manipulation regulate cellular tension independently of Rac activity levels. Blebbistatin (30 μM) downregulates average traction force per microneedle even in the presence of RacV12, whereas phosphomimetic myosin upregulates average traction force, even in the context of reduced Rac activity (NSC23766 treatment). * $p < 0.05$, indicates comparison against RacV12; and # $p < 0.05$, indicates comparison against NSC23766.

(**K-M**) Interdependence of Rac-induced and tension-induced AJ assembly. Inhibition of myosin activity (blebbistatin, 30 μM) reduced the growth of AJs stimulated by constitutively active Rac (RacV12). Loss of Rac activity reduced the growth of AJs stimulated by phosphomimetic myosin. AJs visualised by β-catenin localization. (**L,M**) Effects of double Rac/myosin manipulations in (**J**) on AJ-T_c relationship.

(**N, O**) Rac and tension-dependent pathways control the size of AJs in monolayer culture. Representative immunofluorescent micrographs of monolayers of cells exposed to the treatments in (**G-M**). AJs are visualized by β-catenin staining **(N)**. Quantification of changes in junction size in monolayers (**O**). * $p < 0.05$, indicates comparison against Ctrl; # $p < 0.05$, indicates comparison against RacV12; Δ $p < 0.05$, indicates comparison against NSC23766.

(**P**) Schematic of how myosin-mediated tugging force and Rac activity coordinate to determine the ultimate size and stability of AJs. Our data suggest three general regimes: a low stress regime (shaded green) wherein high Rac activity support AJs assembly

independently of tugging force, a moderate stress regime (white region) wherein Rac activity and myosin-mediated tugging force coordinate to mediate mechano-sensitive growth of AJs, and a high stress regime (shaded red) wherein high tugging forces/myosin activity initiate breaking/disassembly of junctions due to insufficient Rac-mediated junction assembly. All scale bars are 10 μm. Error bars on all graphs denote standard error of the mean.

2.3.4. Microinjection of Constitutively Active RhoA and Direct Mechanical Pulling Leads to Junction Assembly.

While the aforementioned studies argue that tugging forces cause AJ assembly, the reliance on myosin manipulations cannot preclude indirect effects of these manipulations on cortical actin assembly. Moreover, single end-point studies do not provide any insights into the temporal coupling of these phenomena. To address these shortcomings, we characterized the response of AJs in living cells in which only one cell is induced to increase contractility against another, unmanipulated cell. Microinjection of one cell within a bowtie pair with activated Rho protein (RhoA-Q63L) produced an immediate and robust increase in both traction forces (the non-injected cell shows a delayed response) and F_C (Fig. 5B,D), whereas no effect was observed upon microinjection of wild-type RhoA (Fig. 5A,C). Importantly, activated RhoA triggered AJ growth, as revealed by GFP-VE-cadherin localization, within minutes of rising F_C (Fig. 5E,F). This AJ growth was abrogated by inhibition of cytoskeletal tension with Y27632 (Fig. 5F). To confirm whether mechanical force is truly sufficient to promote junction growth, we also placed a micropipet onto one of the cells within the bowtie pair, and pulled, to apply an exogenous tugging force (Fig. 5G). Mechanical loading of the cell-cell junction also promoted VE-cadherin assembly within several minutes of tugging (Fig. 5G,H). These data provide direct evidence that adherens junction assembly responds to cell-cell forces.

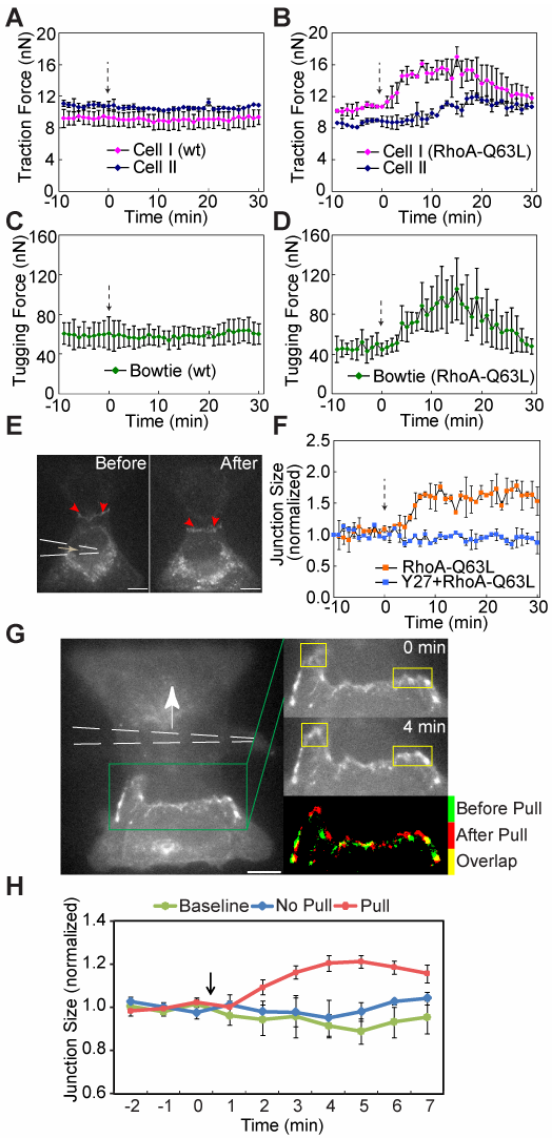

Figure 5. Microinjection of constitutively active RhoA and direct mechanical pulling leads to junction assembly

(**A, B**) Time-series plots showing that traction force does not change in response to microinjection of wild-type Rho protein (wt) (**A**), but is strongly enhanced by constitutively active Rho protein (RhoA-Q63L) (**B**), for each of the two cells in bowtie pairs. Dotted arrow indicates the time point of microinjection, and only Cell I (purple

line) was microinjected. Whiskers show the range of traction force observed in two independent bowtie movies.

(**C, D**) Microinjection of wild-type Rho protein had no effect on tugging forces (**C**); however, tugging forces were acutely increased following microinjection of RhoA-Q63L (**D**). Dotted arrow indicates the time point of microinjection. Whiskers show the range of two replicated experiments across all time points.

(**E**) Representative image frames showing assembly of GFP-VE-cadherin following microinjection of RhoA-Q63L, 10 minutes before and 16 minutes after microinjection, respectively. Dotted white lines indicate the location of the pipette and the red arrow heads point to locations of increased AJ size. Scale bar is 10 μm.

(**F**) RhoA-Q63L induced AJ assembly in a tension-dependent manner. The RhoA-microinjected pairs (orange squares) showed an increase in junction size while pretreatment with Y27632 (25 μM) blocked this effect (blue squares). Dotted arrow indicates the time point of microinjection. Whiskers show the range of two replicated experiments across all time points.

(**G**) Exogenous tugging force stimulated VE-cadherin assembly. Fluorescence micrograph of GFP-VE-cadherin distribution before mechanically pulling the cell-cell junction using a micropipet. Dotted white lines indicate the location of the pipette and the white arrow points to the direction of pipette movement. Region of interest (green box) shows distribution of junctional VE-cadherin before (0 min) and after pulling (4 min), pseudocolored green and red, respectively in the overlay image. Yellow boxes

denote the regions of the AJ showing the strongest cadherin recruitment. Scale bar is 10 μm.

(**H**) Quantification of AJ growth in response to mechanical pulling. AJ size of bowtie pairs over ten minute intervals plotting for baseline (green line), with pipette on top of the cell but no pulling (blue line), or before and after pulling one cell of the bowtie (red). Black arrow indicates the time point of pulling with the micropipet. Whiskers show the standard error of the mean across six independent experiments.

2.4 Discussion

Here we demonstrate that cells generate substantial tugging forces on cell-cell junctions. Previous studies have measured externally applied forces necessary to break or induce changes at the cell-cell adhesion (Potard, Butler et al. 1997; Ko, Arora et al. 2001; Chu, Thomas et al. 2004). While externally applied forces are relevant in numerous biological contexts, here we show that endogenous stresses are experienced between cells even in the absence of such applied forces. Such internal stresses are thought to be critical in morphogenesis, mechanical integrity, and in generating gradients of mechanical stresses to regulate patterns of cell function (Ingber 2003; Scott and Stainier 2003; Nelson, Jean et al. 2005). Thus, further characterizing how such tugging forces are regulated in different settings may be important.

Interestingly the cell-cell junctions appear to dynamically adjust in response to these tugging forces. While previous studies have suggested a requirement for myosin II in maintenance of basal AJ size (de Rooij, Kerstens et al. 2005; Shewan, Maddugoda et al. 2005; Miyake, Inoue et al. 2006; Ivanov, Bachar et al. 2007; Yamada and Nelson 2007; Abraham, Yeo et al. 2009), here we show that activated myosin as well as direct application of exogenous tugging forces induces AJ assembly that occurs within minutes of force application. Mechanosensitive growth of AJs has been proposed based on studies of adhesion to surface-immobilized cadherin ectodomains (Delanoe-Ayari, Al Kurdi et al. 2004; Bard, Boscher et al. 2008). Our data suggest that mechanosensitive growth is a fundamental mechanism for controlling AJ size, and is strikingly similar to

what occurs at focal adhesions (Dembo and Wang 1999; Balaban, Schwarz et al. 2001; Tan, Tien et al. 2003). As has been proposed for focal adhesions, the physiologic consequences of this force-dependent growth are likely twofold. First, force-induced growth of AJs dissipates mechanical stress, and may protect the junction against breakage. Second, AJs are molecular signaling hubs (Erez, Bershadsky et al. 2005), and force-induced junction assembly may trigger signaling that contributes to the process of mechanotransduction. Several models have been proposed to suggest a role for force in AJ assembly. One proposes that localized myosin activation at the expanding edges of cell-cell contacts facilitates zippering the two cell edges together, and thus facilitates AJ growth (Yamada and Nelson 2007). This model requires forces that are parallel to the junction, while our measurements demonstrate forces in a normal direction. An alternative push-pull model (Brevier, Montero et al. 2008) suggests that normal tugging forces may stabilize filopodial-like protrusions that extend along the length of the AJs. Alternatively, mechanical force may alter cadherin clustering or trafficking, parameters that are critical for AJ stability (Yap, Crampton et al. 2007), or may act upon AJ dynamics via conformational changes in mechanically-sensitive cytoskeletal proteins (Bershadsky, Balaban et al. 2003). Regardless, our data reveal a role for Rac1 in modulating the AJ assembly response to force, and underscores the complex and adaptive interplay between signaling, mechanical forces, and junctional structure.

Not only do tugging forces regulate cell-cell adhesions, but in turn cell-cell adhesion assembly can trigger many signals including the Rho GTPases to regulate

cellular mechanics (Fukata and Kaibuchi 2001; Nelson, Pirone et al. 2004). This interplay between force and adhesion highlights how channeling of actomyosin-generated traction and tugging forces at the cell-matrix and cell-cell interface provide a means to dynamically reorganize cell-matrix and cell-cell adhesions locally, as well as the architecture of tissues globally, and further support coordinated crosstalk between the two mechanical interfaces of the cell with its external environment. Understanding the balance between forces across each of these two interfaces ultimately may help to explain multicellular reorganizations such as occur during tissue morphogenesis (Johannes Holtfreter 1944; Warren H. Lewis 1947; Keller, Davidson et al. 2003), and demonstrates the need for better approaches to describe these forces.

CHAPTER III: MECHANICAL FORCES IN ENDOTHELIAL CELLS DURING FIRM ADHESION AND EARLY TRANSMIGRATION OF HUMAN MONOCYTES

3.1 Background

The endothelial cell monolayer controls the passage of molecules and leukocytes into and out of the bloodstream. Such dynamic barrier function plays a critical role in tissue maintenance and repair, angiogenesis, and inflammation. During both innate and adaptive immune responses, the trans-endothelial migration (TEM, also known as extravasation or diapedesis) of leukocytes across the endothelial barrier is a tightly controlled process involving multiple steps. Initially, in response to the inflammatory signal, such as Tumor necrosis factor- α (TNF-α), leukocytes in the bloodstream slow down and start rolling on the endothelium apical surface (Panes, Perry et al. 1999). The subsequent recognition of various chemokines triggers the firm attachment of leukocyte integrins to the adhesion molecules on endothelial cells, such as ICAM-1 (intercellular adhesion molecule-1) and vascular endothelial cell adhesion molecule (VCAM-1) (Boyd, Wawryk et al. 1988; Osborn, Hession et al. 1989; Argenbright, Letts et al. 1991; Bochner, Luscinskas et al. 1991; Springer 1994). This firm adhesion allows the leukocytes to crawl around locally, at or near cell-cell junctions, and finally locate a site to migrate across the endothelium at both junctional and non-junctional locations (Rao, Yang et al. 2007). Failure of the appropriate control of these steps is associated with many pathological conditions, such as chronical inflammatory disorders, metastasis, and atherosclerosis (Desideri and Ferri 2005; Maslin, Kedzierska et al. 2005; Braunersreuther and Mach 2006; Kaneider, Leger et al. 2006).

While we already have a plenty of knowledge of the molecular signals involved in rolling, adhesion, and even transmigration (Petri and Bixel 2006; Vestweber 2007), we are just starting to unveil the mechanical signals in this process and their coordination with molecular signals. It has been indicated that neutrophils generate mechanical force to regulate their motility through actin polymerization and myosin II activation (Eddy, Pierini et al. 2000; Pollard and Borisy 2003). A recent study has characterized the tangential forces exerted by neutrophils during transmigration (Rabodzey, Alcaide et al. 2008). These studies have focused on the mechanical force in leukocytes, but the changes of mechanical force in endothelial cells, especially after firm adhesion, has never been directly measured and characterized. This potential mechanotransduction process inside endothelial cells allows the endothelial cells to actively facilitate the leukocytes to transmigrate through subsequently.

The key step during the above process is the firm adhesion of leukocytes to the endothelial surface, which ends the rolling process and starts the positioning of the leukocytes to the final locations on the endothelial cells for transmigration. There're increasing evidences indicating that endothelial cells could also actively adapt themselves to assist transmigration. Actually, it has been reported that during firm adhesion, cell adhesion molecules could differentially regulate the activity of small Rho-family GTPases to reorganize the endothelial actin cytosckeleton and restructure the cell-cell junctions (Etienne, Adamson et al. 1998; Wojciak-Stothard, Williams et al. 1999; Cook-Mills, Johnson et al. 2004; van Buul and Hordijk 2004; Millan and Ridley 2005;

Cernuda-Morollon and Ridley 2006). Especially, ICAM-1 and VCAM-1 clustering can activate Rac1/ROS and Rho/ROCK pathways, respectively, to induce stress fibre formation and disassembly of VE-cadherin to assist the subsequent transmigration (Thompson, Randi et al. 2002; Alevriadou 2003; van Wetering, van den Berk et al. 2003). However, none of these studies have directly characterized the mechanical force during this process. It would be crucial to see whether the activation of endothelial cell adhesion molecules, such as ICAM-1 or VCAM-1, is sufficient to change the mechanical force in endothelial cells.

Herein, we describe a method to measure the spatial distribution of mechanical force of endothelial cells in a confluent monolayer during firm adhesion and transmigration of human monocyte, using our microfabricated post array force detector system. Briefly, endothelial cells were grown to form confluent monolayers with pre-defined geometries on substrates containing arrays of vertical elastomeric microneedles whose deflections report cellular traction forces. The use of pre-defined geometries actually allows us to consistently characterize and compare changes in mechanical force of the whole endothelial monolayer. Then we triggered the inflammatory response on the endothelial cells, introduced monocytes into the system, and subsequently allowed them to firmly adhere and transmigrate through the endothelial monolayers. By comparing mechanical forces in endothelial cells before and after leukocyte adhesion, we have observed an increase in the traction force of the whole endothelial monolayer during firm adhesion of monocytes. Specifically, the endothelial cell with the monocyte firmly

adhered on it showed a much larger traction force, with the direction of the traction force aligned more centripetally toward the location of firm adhesion. Moreover, activation of ICAM-1 or VCAM-1 molecules on the endothelial cells is sufficient to cause increase in mechanical force of endothelial cells.

3.2 Materials and Methods

3.2.1 Preparation of Substrates

Elastomeric microposts array substrates were fabricated via polydimethylsiloxane (PDMS; Sylgard 184, Dow-Corning, Midland, MI)-based replica-molding and patterned with fibronectin by micro-contact printing as described previously (Tan, Tien et al. 2003). The fibronectin (BD Biosciences, San Jose, CA) patterns consisted of square-shaped regions each with a total area of 10000 μm^2 and coverage of ~120 microposts. Subsequently, microposts were fluorescently labeled with 5 μg/ml Δ^9-DiI (1,1'-dioleyl-3,3,3',3'- tetramethylindocarbocyanine methanesulfonate; Invitrogen, Carlsbad, CA). Cell adhesion was restricted to the squares by blocking the unprinted surface with 0.1% Pluronics F127 (BASF, Mount Olive, NJ).

3.2.2 Cell Culture and Reagents

Human pulmonary artery endothelial cells (HPAECs, Lonza, Basel, Switzerland) were cultured in EGM-2 complete medium (Lonza) supplemented with 10% fetal bovine serum (Sigma, St. Louis, MO). Cells were seeded onto substrates in normal serum-containing media and allowed to spread and grow to form confluent monolayers on post arrays with pre-defined geometries for 36 hours before fixation or further treatment. Human monocytic THP-1 cells were purchased from American Type Culture Collection (Rockville, MD) and grown in RPMI-1640 medium (Sigma) with supplements. To activate HPAECs for adhesion of THP-1 cells, we incubated them with TNF-α (25ng/mL, Roche, USA) for 6 hours prior to introduction of THP-1 monocytes. For fluorescence imaging, prior to being introduced to endothelial monolayers, THP-1 cells were treated with Cell Tracker^{TM} Green (Invitrogen, Carlsbad, CA) at 1:5000 dilution for 30 minutes for fluorescently labeling. All images were taken from Zeiss microscope with Apotome Z-stack imaging acquisition system. Antibodies used for immunofluorescence labeling (and sources) included: mouse anti-β-catenin (BD Biosciences, San Jose, CA), β-catenin (BD Biosciences, San Jose, CA).

3.2.3 Immunofluorescence and Image Analysis

Cells were fixed in 4% paraformaldehyde, blocked in goat serum, incubated with antibody against β-catenin (BD Biosciences, San Jose, CA) and then detected with fluorophore-conjugated isotype-specific anti-IgG antibodies (Invitrogen, Carlsbad, CA). Cells were also labeled with AlexaFluor-488-conjugated Phalloidin and Hoescht33342 (Invitrogen, Carlsbad, CA). Fluorescence images were acquired on a Zeiss Axiovert 200M with 40× oil objective (Zeiss MicroImaging, Thornwood, NY) and processed in Matlab to quantify mechanical force.

3.2.4 Measurement of Traction Forces

Fluorescence images were taken of the microposts at focal planes passing through the tips and base, using an Axiovert 200M (Zeiss MicroImaging, Thornwood, NY) equipped with an Apotome module to remove out-of-focus fluorescence signals. The centroids of the microposts at both planes were determined by localized thresholding using an automated Matlab program (Mathworks, Natick, MA). After performing image registration on the tip and base centroids, the force on each post was computed by multiplying the deflection by the spring constant of the post, which is 64 nN/μm. Adherens Junction staining was used to identify which microposts were attached to each cell in a monolayer.

3.2.5 Beads Preparation and Adhesion Experiment

The beads were prepared as described before (Allingham, van Buul et al. 2007). Briefly, anti-ICAM-1, anti-VCAM-1, and IgG mAbs were purchased from R&D Systems. Three-micron polystyrene beads were purchased from Polysciences and were pretreated overnight with 8% glutaraldehyde, washed five times with PBS, and incubated with 300 μg/ml ICAM-1, VCAM-1 or IgG mAb according to the manufacturer's protocol.

3.2.6 Statistical Analysis

Data are expressed as mean ± s.e.m. or mean ± s.d. as indicated in the figure legends. Linear regression and Student's t-test were performed for statistical analysis. Zonal analysis was performed using an automated program coded in MATLAB (Mathworks, Natick, MA). Briefly, the zones were generated by dilation from the microposts underneath the monocytes in "local" to "distant" zonation, and erosion from the outermost layer of microposts in "edge" to "interior" zonation, respectively. Due to the square shape of monolayers, 8-nearest neighbor dilation/erosion was used to generate the zones. To compare "local" to "distant" zones with the Ctrl and TNF conditions, ghost monocyte locations were generated using Matlab to compute a uniform distribution across the endothelial monolayers. Applying a Kolmogorov-Smirnov Test indicated no significant differences between the sample and ghost monocyte distributions ($p = 0.99$ and 0.43 for comparisons on x- and y-coordinates, respectively). The histograms in relative angle analysis in Fig. 7d, f were fit with a Gamma distribution with nonlinear least square methods for TEM conditions, or with an average line for Ctrl and TNF conditions. The pseudo-color plot for traction forces in Fig 8a was filtered and smoothed with a bi-cubic 2D spatial filter in Matlab.

3.3 Results

3.3.1 Approach to Measure Traction Force in Endothelial Monolayers during Monocyte Recruitment

Endothelial cells were seeded and allowed to spread and grow to form confluent monolayers with pre-defined geometries on substrates containing arrays of vertical elastomeric microposts whose deflections report cellular traction forces (Fig. 6a). To be consistent in the comparisons between different conditions and treatment, we fixed the geometry of endothelial monolayers by microcontact-printing of fibronectin (FN) on 100um×100um square regions on posts for all subsequent experiments.

Endothelial cells were allowed to form mature cell-cell junctions and fully spread into the square FN-coated regions on posts for 36 hours, and then treated with TNF-α to induce expression of the ICAM-1 and VCAM-1 required for monocyte adhesion. After 6 hours of incubation with TNF-α, we then introduced monocytes (THP-1 cells) into the system and allowed them to roll on, firmly adhere to, and finally transmigrate across the activated endothelial monolayers. After initial adhesion, the monolayers were rinsed to remove monocytes not firmly bound, fixed, and processed for immunofluorescence imaging. In the absence of TNF-α treatment, monocyte adhesion was virtually undetectable, while in the presence of TNF-α, monocyte adhesion was robust and reproducible. Using optical sectioning to image samples, the vertical position of monocytes with respect to the associated endothelial monolayers could be measured. Monocytes were found at multiple z-axis planes including slightly above, co-planar, and

slightly underneath the endothelial plane, consistent with the presence of firmly adherent as well as transmigrating stages of monocytes (Fig. 6b). We restricted all subsequent studies to cases in which the z-plane with the strongest fluorescent signal for monocytes were in the same plane with the endothelial cells (0μm) or underneath endothelial cells (−3μm) (Fig. 6c). Operationally, we defined firm adhesion as the population of monocytes that remain attached after a washing step but do not protrude below the endothelial monolayer. Because firm adhesion is followed by transmigration and this transition is gradual, we defined firm adhesion (TEM-F.A.) when the main monocyte body was above the monolayer (0 and +3μm), even though it can still protrude partially into the endothelial monolayer. We defined early transmigration (TEM-E.T.) conversely, when a larger portion of the cell was one layer below the monolayer plane (0 and -3 μm).

By carefully controlling the density of monocytes and the timing of washing-off and fixation, we focused only on monolayers exhibiting either one or zero monocyte firmly adhered/transmigrating on it before fixation (Fig. 6d, e), which allowed us to consistently compare the forces in endothelial monolayers with or without monocytes on it.

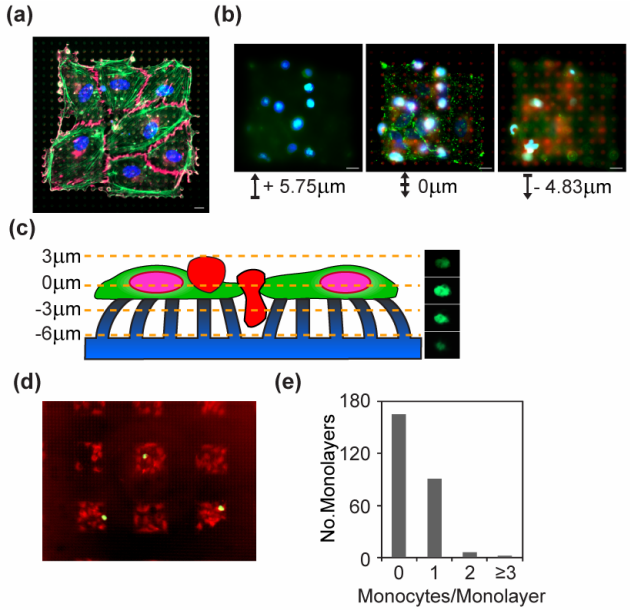

Figure 6. Approach to measure traction force in endothelial monolayers during monocyte adhesion and early transmigration

(a) Endothelial cells grown on mPADs (Monolayer size: 150µm×150µm). Immunofluorescence staining indicates cell nucleus (blue), actin filaments (green), micro-posts (gray), and β-catenin (magenta), respectively.

(b) Endothelial cell monolayers grown on mPADs with monocytes transmigrating through them. Images taken from focal plane 5.75 µm above, 0 µm, and 4.83 µm below the monolayer. Immunofluorescence staining indicates endothelial cell nucleus (dark blue), monocytes (bright cyan), micro-posts (red), and β-catenin (green) (monolayer size: 100µm×100µm).

(c) Schematic figure for monocyte firm adhesion and early transmigration on endothelial cells on posts. The fluorescence images on the right are cell-tracker green staining at different focal planes of the monocyte transmigrating on an endothelial monolayer.

(d) Array of endothelial monolayers showing each monolayer has 1 or 0 monocytes transmigrating on it.

(e) Histogram showing most of the endothelial monolayers have 1 or 0 monocyte on it. Scale bars indicate 10μm.

3.3.2 Traction Forces Reported During Firm Adhesion and Early Transmigration

Traction forces were obtained for endothelial monolayers in untreated control, TNF-α-treated, and transmigration conditions (Fig. 7a). By quantifying the average magnitude of traction forces across each monolayer as a measure of average endothelial contractility, we observed a slight increase in TNF-α-treated cells and a large increase in the monolayers with monocytes in either firm adhesion or early transmigration stages (Fig. 7b). Because we did not observe significant differences in endothelial mechanics between firm adhesion and early transmigration conditions, we did not distinguish these two cases and instead refer to both as "trans-endothelial migration" (TEM), treating them as one group in all subsequent quantifications. These data indicated that the monocytes appear to induce a change in the mechanics of the monolayer.

We postulated that one possible effect of monocyte adhesion would be to either induce endothelial cells to generate traction forces to pull away from the monocyte (allowing retraction and opening of a hole for monocytes pass through the monolayer) or to pull centripetally toward the monocyte (perhaps acting to anchor and stabilize monocyte adhesion with additional actin stress fiber connections). To investigate these possibilities, we quantified the degree of re-alignment of traction forces in the endothelial cells, with respect to the position of the monocyte on the monolayer. We defined a relative angle (Rel. Angle) between the traction force vector for any particular micropost and the centripetal line connecting the centroid of the monocyte to the micropost location (Fig. 7c). Here, zero degree denotes a force vector pointing toward the monocyte. The

histogram of the relative angles for all of the monolayers indicated a small bias at lower angles in the non-treated monolayers (Ctrl), which reflected an expected intrinsic centripetality of forces toward the centroid of the non-treated monolayer. Interestingly, this intrinsic bias was lost when monolayers were treated with TNF-α, and introduction of monocytes led to a pronounced peak near zero angle (Fig. 7d), which indicated a re-direction of traction forces in the endothelial monolayer guided toward the centroid of monocyte adhesion.

Previous studies have indicated that after firm adhesion of monocytes, the endothelial cell directly contacting the monocyte weakens their cell-cell junctions to prepare for the monocytes to transmigrate through between them (Allport, Ding et al. 1997; Allport, Muller et al. 2000; Shaw, Bamba et al. 2001; Kataoka, Iwaki et al. 2002; Ionescu, Cepinskas et al. 2003; van Wetering, van den Berk et al. 2003). Thus, we categorized the endothelial cells in our dataset into two subgroups: the endothelial cell directly contacting the monocyte (Ct) and all of the rest of the endothelial cells not directly contacting the monocyte (NCt) (Fig. 7c). For monocytes spanning more than one endothelial cell, we defined the Ct cell as the one with the largest contacting area with the monocytes. We then performed the analysis of traction forces as above (Fig. 7e-f). We observed much larger and more centripetal traction force in the monocyte-contacting endothelial cells, though we still observed a significant but smaller increase in magnitude and re-orientation of traction forces in the rest of the endothelial cells not contacting the monocytes (Fig. 7e-f). Together, these results indicated that monocytes transmigrating on

endothelium induce substantial increases in traction forces within the endothelial monolayer. These effects are most pronounced in the endothelial cell in direct contact with the monocyte, but importantly are also propagated to the surrounding endothelial cells within the same monolayer.

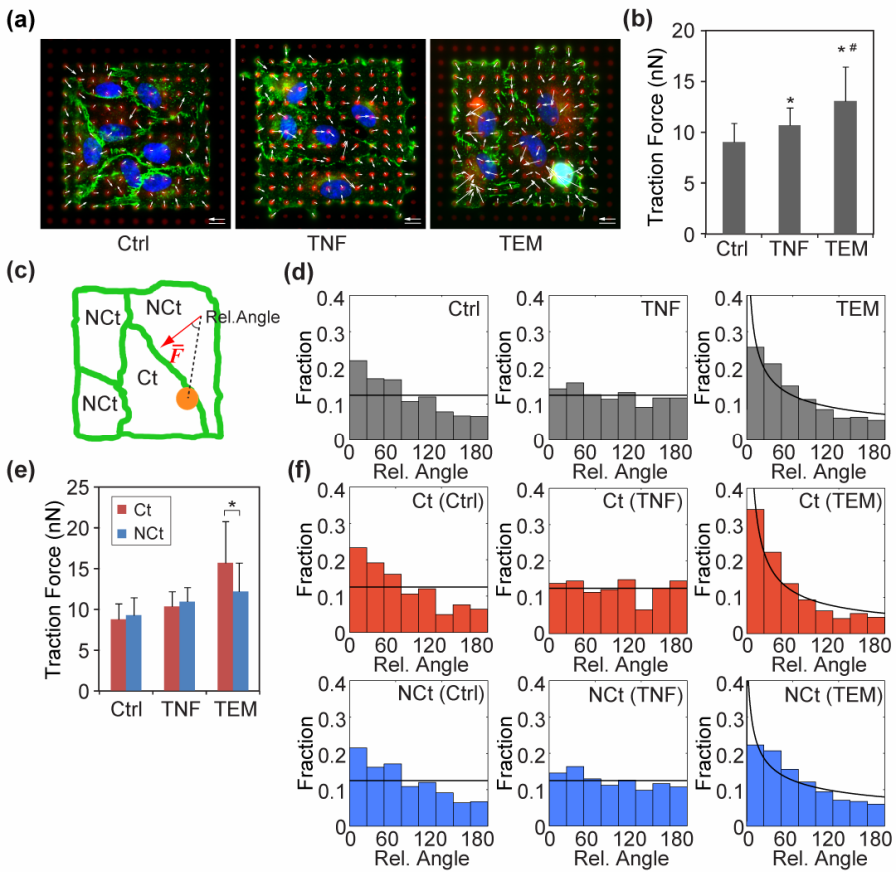

Figure 7. Traction forces reported during firm adhesion and early transmigration

(a) Fluorescence images showing endothelial monolayers at baseline (Ctrl), TNFα-treated (TNF), and with monocyte transmigrating on it (TEM), respectively. Immunofluorescence staining indicates beta-catenin (green); and monocyte (bright cyan); nucleus (blue); microposts (red). Scale bars indicate 10μm; white arrows in figures indicate the vector of traction forces with scaled arrow bar indicating 32 nN.

(b) Bar graph indicating increase in average traction force in endothelial monolayers with monocytes transmigrating on them. * $p < 0.05$, indicates comparison against Ctrl; # $p < 0.05$, indicates comparison against TNF;

(c) Definition of the relative angle (Rel. Angle): the angle (absolute value, in degrees) between the traction force vector of each location on the endothelial monolayer and the centripetal line connecting the center of the monocyte to that location; and also the definitions of Ct Endo and NCt Endo, as the endothelial cell directly contacting the monocyte, or not, respectively. For monocytes spanning more than one endothelial cell, we defined the Ct cell as the one with the largest contacting area with the monocytes.
(d) Histograms showing the distribution of Rel. Angle for Ctrl, TNF, and TEM conditions. The TEM condition was fit with gamma distribution (see Methods). See Methods for how ghost monocyte locations were generated for Ctrl and TNF conditions.
(e) Bar graph indicating a significant difference in average traction forces between Ct and NCt cells in the TEM condition. * $p < 0.05$, indicates comparison against Ct.
(f) Histograms showing the distribution of Rel. Angle in both Ct and NCt cells for Ctrl, TNF, and TEM conditions. Ctrl and TNF are fit with uniform distribution and TEM is fit with gamma distribution.
All error bars indicate standard deviation.

3.3.3. Spatial Distribution of Traction Forces in Endothelial Monolayer during Firm Adhesion and Early Transmigration

Although there was a more pronounced stimulation of traction force in the endothelial cell in direct contact with the monocyte, we considered the possibility that the stimulatory mechanical effect was even more localized than just defined by cell boundaries: Replotting Fig. 7a revealed local peaks in contractile force that were not defined by the boundaries of cells, but much smaller regions. Indeed, it appeared that there was a peak in force in a small subcellular region directly underneath the monocyte (Fig. 8a).

In order to extend this observation across our entire dataset, we refined the force analysis by segmenting the monolayer into zones from "local" to "distant" relative to the location of monocyte (Fig. 8b). Then, we obtained the average traction forces for every zone in the monolayer and compared it across different conditions. This analysis revealed a significant increase in local contractility in the endothelial cells with respect to the transmigrating monocyte (Fig. 8c), and is consistent with reports of actin remodeling locally around the position of monocyte firm adhesion (Etienne, Adamson et al. 1998; van Buul, Allingham et al. 2007).

We also tested whether there might be differences in average traction forces near the edges versus interior of monolayers as has been suggested by previous studies (Nelson, Jean et al. 2005), by segmenting the monolayer into zones from "edge" vs. "interior" zones (Fig. 8d). Slightly larger traction forces appeared to exist at the edges as

compared to the interior zone for both baseline and transmigrating monolayers, but the trend was not significant ($p > 0.10$) (Fig. 8e).

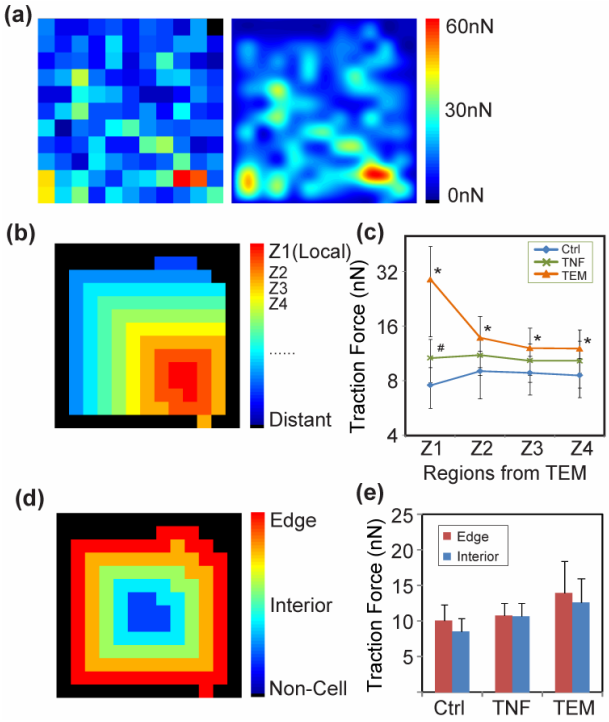

Figure 8. Spatial distribution of traction forces in endothelial monolayer during firm adhesion and early transmigration

(a) The magnitude of traction forces in the transmigration monolayer in Fig. 7a was re-plotted in pseudo-color, filtered and smoothed with a bi-cubic 2D spatial filter.

(b) Zones from "Local" to "Distant" relative to the location of monocyte. Z1 is the zone of posts in the closest vicinity around the monocyte, Z2 next closest, Z3…and so on. The segmentation was performed on the transmigrating monolayer in Fig. 7a.

(c) Average traction force in each zone as defined in **(b)** compared across all conditions. * or #, $p < 0.05$, indicates comparison against Ctrl at each zone.

(d) Zones from "Edge" to "Interior". "Edge" is defined as the outmost zone, and

"Interior" is defined as the combination of all the rest of the zones.

(e) Bar graph indicating no significant difference in average traction forces between "Edge" and "Interior" zones as defined in **(d)** in all conditions.

All error bars indicate standard deviation.

3.3.4 Activation of Endothelial ICAM-1/VCAM-1 is Enough to Trigger Increase in Traction Forces

ICAM-1 and VCAM-1 appear to be critical players during firm adhesion-induced transmigration (Thompson, Randi et al. 2002; Alevriadou 2003; van Wetering, van den Berk et al. 2003; Allingham, van Buul et al. 2007). It has been reported that ICAM-1-coated beads were sufficient to mimic ICAM-1 engagement during firm adhesion and trigger downstream intracellular signal pathways required for subsequent TEM (Allingham, van Buul et al. 2007). To test whether engagement of either receptor might be involved in the observed changes in endothelial mechanics observed with monocytes, we exposed endothelial monolayers with polystyrene beads coated with anti-ICAM-1 or anti-VCAM-1 mAb (Fig. 9a). Engagement of ICAM-1 but not VCAM-1 significantly increased average traction force in the monolayer (Fig. 9b), although the increase was not as high as when exposed to monocytes. When comparing traction forces of cells in contact versus non-contact with beads, there appeared to be a slight trend toward increased traction but the effect was not significant (Fig. 9c). However, when using local zones to segment the dataset, one observed a high traction force level in the local zones near either ICAM-1or VCAM-1-coated beads (Fig. 9d). Together, these data suggest that both receptors are involved in the mechanical response of endothelium to monocytes.

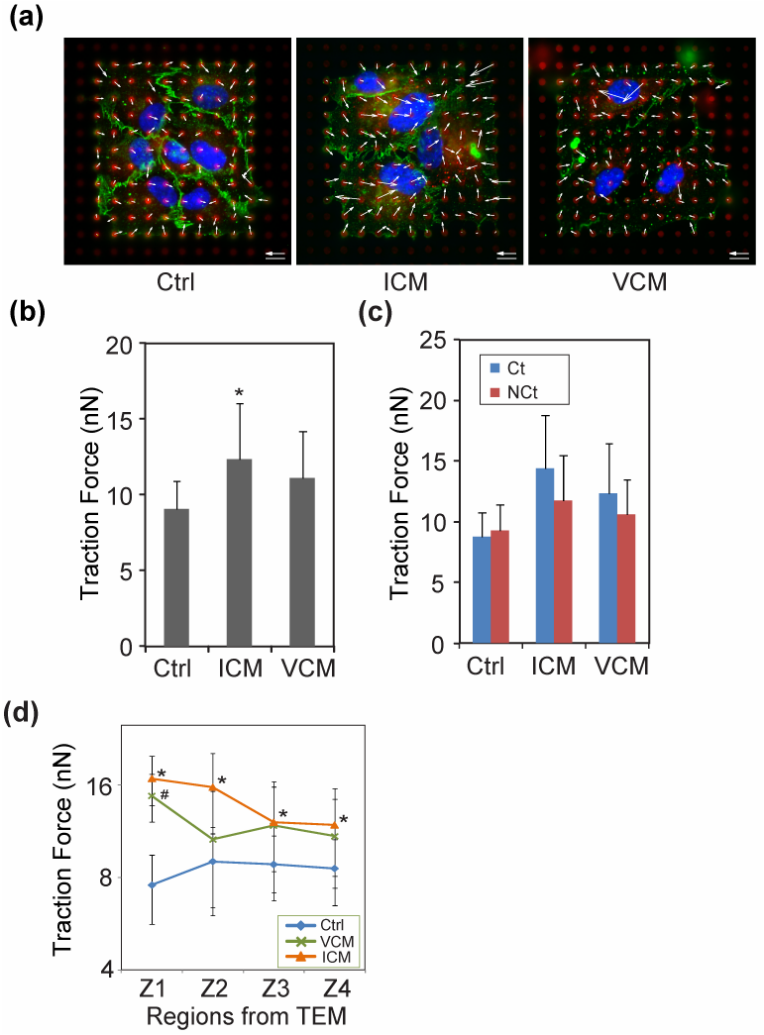

Figure 9. Activation of endothelial ICAM/VCAM-1 is enough to trigger increase in traction forces

(a) Fluorescence images showing endothelial monolayers for baseline (Ctrl), ICAM-1-treated (ICM), and with VCAM-1-treated (VCM), respectively. Green is beta-catenin showing cell-cell junctions; blue is Dapi staining for cell nucleus; red dots are DiI staining for PDMS posts. In the last two image, the bright green circular dots are the

ICAM-1 and VCAM-1-coated beads.

(b) Bar graph indicating increase in average traction force in ICAM-1-treated endothelial monolayers. * $p < 0.05$, indicates comparison against Ctrl.

(c) Bar graph indicating no significant difference in average traction forces between Ct and NCt cells in ICM or VCM condition.

(d) Average traction force in each zone from "Local" to "Distant" relative to the location of monocyte, as defined in Fig. 8d, compared across all above conditions. * or #, $p < 0.05$, indicates comparison against Ctrl at each zone.

All error bars indicate Standard Deviation.

3.4 Discussion

With the use of a microfabricated force measurement system, we report the first characterization of mechanical forces in endothelial monolayers induced by monocyte adhesion and transmigration.

Our results demonstrate an increase in traction forces in endothelial monolayer during firm adhesion and early transmigration. Previous studies have indicated that after firm adhesion of monocytes, the endothelial cell directly contacting the monocyte weaken their cell-cell junctions to prepare for the monocytes to transmigrate through between them (Allport, Ding et al. 1997; Allport, Muller et al. 2000; Shaw, Bamba et al. 2001; Kataoka, Iwaki et al. 2002; Ionescu, Cepinskas et al. 2003; van Wetering, van den Berk et al. 2003). Other studies have shown that vasoactive agents like thrombin induce a rapid and transient activation of RhoA, accompanied by an increase in myosin light chain phosphorylation, the generation of F-actin stress fibers, and a prolonged increase in endothelial permeability (van Nieuw Amerongen, van Delft et al. 2000). In this process, endothelial cells change their cytoskeleton to allow small gaps forming between neighboring cells, potentially to allow molecules and cells to cross through. It is possible that leukocytes can usurp this same pathway for inducing transmigration, by initiating Rho-dependent signaling that in turn activates contractility to promote gap formation (Springer 1994; Worthylake and Burridge 2001; Hordijk 2006; Petri and Bixel 2006) .

Consistent with this link between RhoA signaling and permeability is also the local nature of the effect: transmigrating T-lymphocytes appear to be surrounded by a

microvillus-like docking structure whose formation appears to involve RhoA/ROCK signaling (Barreiro, Yanez-Mo et al. 2002; Carman, Jun et al. 2003). Importantly, abrogation of these structures appears to inhibit transmigration but not firm adhesion. Because ROCK can also induce contractile forces, these observations are consistent with our results of a local increase of traction force in the monolayer at the point of monocyte contact. Understanding the spatiotemporal dynamics of these localized traction forces may provide additional insights into how these mechanochemical signals ultimately impact transmigration.

There are number of studies showing that during firm adhesion, the engagement of endothelial ICAM-1 triggers Rho/ROCK signaling and stress fiber assembly (Etienne, Adamson et al. 1998; Thompson, Randi et al. 2002; van Buul, Allingham et al. 2007). Our results showed an increase in traction force after inducing ICAM-1 but not VCAM-1. One possibility is that VCAM-1 was suboptimally activated using antibody-coated beads. The difference between ICAM-1 and VCAM-1 also could result from the differential involvement of these two factors in different steps of transmigration. VCAM-1 is thought to be involved earlier, including both the rolling and adhesion stages , while ICAM-1 is more restricted to the firm adhesion and transmigration process (Millan and Ridley 2005). The difference in the induced traction force may reflect different requirements for mechanical changes within endothelial cells for these different stages of transmigration**.**

In summary, the studies reported here highlight the intimate, highly dynamic, and

spatially localized mechanical interactions between leukocytes and the endothelial monolayer, that are likely critical to the biophysical process of transmigration. As such, the development of new tools to characterize the mechanics of these events is likely to play a critical role in elucidating the mechanisms by which this dynamic barrier known as the endothelium operates.

CHAPTER IV: CONCLUSIONS AND FUTURE DIRECTIONS

4.1 Conclusions

This thesis focuses on the role of the mechanical forces in multicellular system, specifically on modulating cell-ECM and cell-cell adhesions to regulate endothelial cell organization and function.

First, we have established a novel method to directly measure tugging forces experienced at the cell-cell junctions between neighboring cells. The ability of cell-cell junctions to sustain mechanical loads is critical to maintaining the integrity of tissues and organs, but the mechanical forces at these junctions have never been directly measured. Moreover, combining this novel method with expression of phosphomimetic myosin light chain, knockdown of myosin, and micromanipulation, we discover that myosin-mediated tugging force regulates the size of cell-cell junctions. Further, the mechanism of force-mediated growth requires Rac activity. These results establish a direct link between force and function of adherens junctions, similar to the relationship between traction forces and focal adhesions at the cell-ECM interface, and describe the ability of cells to regulate cell-cell adhesion by modulating this tugging force.

Furthermore, I have extended our approach of measuring mechanical forces in multicellular system to a larger scale involving an endothelial cell monolayer and its interaction with the monocyte adhered and transmigrating on it. I have characterized the mechanical forces in the endothelial monolayer at a cellular, sub-cellular and pan-cellular level with and without monocyte adhesion and transmigration. I have found that the endothelial cells modulated their mechanical force spatially in response to monocyte

adhesion, to potentially facilitate the subsequent transmigration. This is the first time to reveal the mechanical force in endothelial cells during this fundamental physiological process. And the microfabricated tools and quantification methods developed with this project will inspire the future research in this area.

While these studies were demonstrated in endothelial cells, the conclusions linking mechanical forces and physiology of cell-cell adhesions and immune response like transmigration are of general interests, and have fundamental importance of multicellular forces in numerous physiological and pathological processes, I believe that my work in this thesis will be of general interest to the scientific community.

4.2 Future Directions

4.2.1. Force-Ome: to Explore the Systems Biology of Cell Mechanics

Previously, most of the studies have been focusing on the qualitative understanding of single signal molecules that are responsible for cellular contractility, which lacks the predictive power. Therefore, to get a more systematic understanding of cellular contractility, an important question remains to be answered is whether different activation profiles of cellular contractility triggered by distinct extracellular stimuli can be *predicted quantitatively* by the ability of these stimuli to activate specific signal transduction pathways. Diverse extracellular stimuli can converge on shared intracellular networks/circuitry, and mediate stereotypical responses. Statistical models aim to address questions of how proteomic networks control these cellular responses, for example the cellular contractility dynamics, through exploratory data analysis (Janes, Albeck et al. 2005; Janes and Lauffenburger 2006; Bakal, Aach et al. 2007). Therefore, one potential direction is to use automated measurement tools (such as mPADs combining with automated imaging acquisition and processing programs) and statistical methods to identify the molecular signals that are responsible for various cellular force signatures in response to different extracellular stimuli. One example would be performing a PLS-based supervised decomposition to reduce the signaling vector space into principal components (Janes, Albeck et al. 2005; Janes and Lauffenburger 2006) and determine which signal/input combinations contain essential signaling information for predicting contractility.

4.2.2. Theoretical Studies of Monocyte-Induced Force Redistribution

In the Transmigration study, I have analyzed the spatial re-distribution of the magnitude and orientation of traction forces in endothelial monolayers during monocyte firm adhesion and transmigration. The Rel. Angles in monocyte-arrested monolayer showed a nice Gamma distribution in both Ct and NCt cells. A very interesting direction is to understand the profile of the effect of the monocyte adhesion to the endothelial monolayer, and how it propagates across multiple cells to the distant zones of the monolayer, and why it fit with Gamma distribution. One of the possibilities is that Gamma distribution actually reduced to Exponential distribution, which is possibly due to the cumulative effect of large number of random traction force vectors perturbed by a centripetal force by the monocytes. If the monocyte is a pure physical object, we can assume a passive long range effect across the monolayer and simulate the final re-distribution map of vectors after that. However, monocyte is not merely a physical object. Thus, by simulation, it's possible to calculate back the actually effective profile of monocyte across long distance, which will eventually give us some quantitative clue on how the molecular signals activated by the monocyte adhesion is transmitted physically across multiple cells.

BIBLIOGRAPHY

Abraham, S., M. Yeo, et al. (2009). "VE-Cadherin-mediated cell-cell interaction suppresses sprouting via signaling to MLC2 phosphorylation." Curr Biol **19**(8): 668-74.

Adams, C. L., W. J. Nelson, et al. (1996). "Quantitative analysis of cadherin-catenin-actin reorganization during development of cell-cell adhesion." J Cell Biol **135**(6 Pt 2): 1899-911.

Alevriadou, B. R. (2003). "CAMs and Rho small GTPases: gatekeepers for leukocyte transendothelial migration. Focus on "VCAM-1-mediated Rac signaling controls endothelial cell-cell contacts and leukocyte transmigration"." Am J Physiol Cell Physiol **285**(2): C250-2.

Allingham, M. J., J. D. van Buul, et al. (2007). "ICAM-1-mediated, Src- and Pyk2-dependent vascular endothelial cadherin tyrosine phosphorylation is required for leukocyte transendothelial migration." J Immunol **179**(6): 4053-64.

Allport, J. R., H. Ding, et al. (1997). "Endothelial-dependent mechanisms regulate leukocyte transmigration: a process involving the proteasome and disruption of the vascular endothelial-cadherin complex at endothelial cell-to-cell junctions." J Exp Med **186**(4): 517-27.

Allport, J. R., W. A. Muller, et al. (2000). "Monocytes induce reversible focal changes in vascular endothelial cadherin complex during transendothelial migration under

flow." J Cell Biol **148**(1): 203-16.

Argenbright, L. W., L. G. Letts, et al. (1991). "Monoclonal antibodies to the leukocyte membrane CD18 glycoprotein complex and to intercellular adhesion molecule-1 inhibit leukocyte-endothelial adhesion in rabbits." J Leukoc Biol **49**(3): 253-7.

Bakal, C., J. Aach, et al. (2007). "Quantitative morphological signatures define local signaling networks regulating cell morphology." Science **316**(5832): 1753-6.

Balaban, N. Q., U. S. Schwarz, et al. (2001). "Force and focal adhesion assembly: a close relationship studied using elastic micropatterned substrates." Nat Cell Biol **3**(5): 466-72.

Bard, L., C. Boscher, et al. (2008). "A molecular clutch between the actin flow and N-cadherin adhesions drives growth cone migration." J Neurosci **28**(23): 5879-90.

Barreiro, O., M. Yanez-Mo, et al. (2002). "Dynamic interaction of VCAM-1 and ICAM-1 with moesin and ezrin in a novel endothelial docking structure for adherent leukocytes." J Cell Biol **157**(7): 1233-45.

Baumer, Y., D. Drenckhahn, et al. (2008). "cAMP induced Rac 1-mediated cytoskeletal reorganization in microvascular endothelium." Histochem Cell Biol **129**(6): 765-78.

Baumgartner, W., P. Hinterdorfer, et al. (2000). "Cadherin interaction probed by atomic force microscopy." Proc Natl Acad Sci U S A **97**(8): 4005-10.

Bershadsky, A. D., N. Q. Balaban, et al. (2003). "Adhesion-dependent cell mechanosensitivity." Annu Rev Cell Dev Biol **19**: 677-95.

Bertet, C., L. Sulak, et al. (2004). "Myosin-dependent junction remodelling controls planar cell intercalation and axis elongation." Nature **429**(6992): 667-71.

Bochner, B. S., F. W. Luscinskas, et al. (1991). "Adhesion of human basophils, eosinophils, and neutrophils to interleukin 1-activated human vascular endothelial cells: contributions of endothelial cell adhesion molecules." J Exp Med **173**(6): 1553-7.

Boyd, A. W., S. O. Wawryk, et al. (1988). "Intercellular adhesion molecule 1 (ICAM-1) has a central role in cell-cell contact-mediated immune mechanisms." Proc Natl Acad Sci U S A **85**(9): 3095-9.

Braga, V. M. (2002). "Cell-cell adhesion and signalling." Curr Opin Cell Biol **14**(5): 546-56.

Braga, V. M., L. M. Machesky, et al. (1997). "The small GTPases Rho and Rac are required for the establishment of cadherin-dependent cell-cell contacts." J Cell Biol **137**(6): 1421-31.

Braunersreuther, V. and F. Mach (2006). "Leukocyte recruitment in atherosclerosis: potential targets for therapeutic approaches?" Cell Mol Life Sci **63**(18): 2079-88.

Brevier, J., D. Montero, et al. (2008). "The asymmetric self-assembly mechanism of adherens junctions: a cellular push-pull unit." Phys Biol **5**(1): 16005.

Burridge, K., K. Fath, et al. (1988). "Focal adhesions: transmembrane junctions between the extracellular matrix and the cytoskeleton." Annu Rev Cell Biol **4**: 487-525.

Carman, C. V., C. D. Jun, et al. (2003). "Endothelial cells proactively form microvilli-like

membrane projections upon intercellular adhesion molecule 1 engagement of leukocyte LFA-1." J Immunol **171**(11): 6135-44.

Cavallaro, U. and G. Christofori (2004). "Cell adhesion and signalling by cadherins and Ig-CAMs in cancer." Nat Rev Cancer **4**(2): 118-32.

Cernuda-Morollon, E. and A. J. Ridley (2006). "Rho GTPases and leukocyte adhesion receptor expression and function in endothelial cells." Circ Res **98**(6): 757-67.

Chen, C. S., J. Tan, et al. (2004). "Mechanotransduction at cell-matrix and cell-cell contacts." Annu Rev Biomed Eng **6**: 275-302.

Chu, Y. S., W. A. Thomas, et al. (2004). "Force measurements in E-cadherin-mediated cell doublets reveal rapid adhesion strengthened by actin cytoskeleton remodeling through Rac and Cdc42." J Cell Biol **167**(6): 1183-94.

Conti, M. A., S. Even-Ram, et al. (2004). "Defects in cell adhesion and the visceral endoderm following ablation of nonmuscle myosin heavy chain II-A in mice." J Biol Chem **279**(40): 41263-6.

Cook-Mills, J. M., J. D. Johnson, et al. (2004). "Calcium mobilization and Rac1 activation are required for VCAM-1 (vascular cell adhesion molecule-1) stimulation of NADPH oxidase activity." Biochem J **378**(Pt 2): 539-47.

Cullere, X., S. K. Shaw, et al. (2005). "Regulation of vascular endothelial barrier function by Epac, a cAMP-activated exchange factor for Rap GTPase." Blood **105**(5): 1950-5.

Dawes-Hoang, R. E., K. M. Parmar, et al. (2005). "folded gastrulation, cell shape change

and the control of myosin localization." Development **132**(18): 4165-78.

de Rooij, J., A. Kerstens, et al. (2005). "Integrin-dependent actomyosin contraction regulates epithelial cell scattering." J Cell Biol **171**(1): 153-64.

Dejana, E. (2004). "Endothelial cell-cell junctions: happy together." Nat Rev Mol Cell Biol **5**(4): 261-70.

Dejana, E., M. Corada, et al. (1995). "Endothelial cell-to-cell junctions." Faseb J **9**(10): 910-8.

Delanoe-Ayari, H., R. Al Kurdi, et al. (2004). "Membrane and acto-myosin tension promote clustering of adhesion proteins." Proc Natl Acad Sci U S A **101**(8): 2229-34.

Dembo, M. and Y. L. Wang (1999). "Stresses at the cell-to-substrate interface during locomotion of fibroblasts." Biophys J **76**(4): 2307-16.

Desideri, G. and C. Ferri (2005). "Endothelial activation. Sliding door to atherosclerosis." Curr Pharm Des **11**(17): 2163-75.

Dudek, S. M. and J. G. Garcia (2001). "Cytoskeletal regulation of pulmonary vascular permeability." J Appl Physiol **91**(4): 1487-500.

Eddy, R. J., L. M. Pierini, et al. (2000). "Ca2+-dependent myosin II activation is required for uropod retraction during neutrophil migration." J Cell Sci **113 (Pt 7)**: 1287-98.

Erez, N., A. Bershadsky, et al. (2005). "Signaling from adherens-type junctions." Eur J Cell Biol **84**(2-3): 235-44.

Etienne, S., P. Adamson, et al. (1998). "ICAM-1 signaling pathways associated with Rho

activation in microvascular brain endothelial cells." J Immunol **161**(10): 5755-61.

Foty, R. A., C. M. Pfleger, et al. (1996). "Surface tensions of embryonic tissues predict their mutual envelopment behavior." Development **122**(5): 1611-20.

Fukata, M. and K. Kaibuchi (2001). "Rho-family GTPases in cadherin-mediated cell-cell adhesion." Nat Rev Mol Cell Biol **2**(12): 887-97.

Fukuhara, S., A. Sakurai, et al. (2005). "Cyclic AMP potentiates vascular endothelial cadherin-mediated cell-cell contact to enhance endothelial barrier function through an Epac-Rap1 signaling pathway." Mol Cell Biol **25**(1): 136-46.

Gavard, J., M. Lambert, et al. (2004). "Lamellipodium extension and cadherin adhesion: two cell responses to cadherin activation relying on distinct signalling pathways." J Cell Sci **117**(Pt 2): 257-70.

Gumbiner, B. M. (2005). "Regulation of cadherin-mediated adhesion in morphogenesis." Nat Rev Mol Cell Biol **6**(8): 622-34.

Halir, R. and J. Flusser (1998). "Numerically stable direct least squares fitting of ellipses." Proceedings of the 6th International Conference in Central Europe on Computer Graphics and Visualization.: 125-132.

Hordijk, P. L. (2006). "Endothelial signalling events during leukocyte transmigration." Febs J **273**(19): 4408-15.

Huxley, H. E. (1969). "The mechanism of muscular contraction." Science **164**(886): 1356-65.

Ingber, D. E. (2003). "Tensegrity I. Cell structure and hierarchical systems biology." J

Cell Sci **116**(Pt 7): 1157-73.

Ionescu, C. V., G. Cepinskas, et al. (2003). "Neutrophils induce sequential focal changes in endothelial adherens junction components: role of elastase." Microcirculation **10**(2): 205-20.

Ivanov, A. I., M. Bachar, et al. (2007). "A unique role for nonmuscle myosin heavy chain IIA in regulation of epithelial apical junctions." PLoS One **2**(7): e658.

Janes, K. A., J. G. Albeck, et al. (2005). "A systems model of signaling identifies a molecular basis set for cytokine-induced apoptosis." Science **310**(5754): 1646-53.

Janes, K. A. and D. A. Lauffenburger (2006). "A biological approach to computational models of proteomic networks." Curr Opin Chem Biol **10**(1): 73-80.

Johannes Holtfreter (1944). "A study of the mechanics of gastrulation." Journal of Experimental Zoology **95**(2): 171-212.

Kaneider, N. C., A. J. Leger, et al. (2006). "Therapeutic targeting of molecules involved in leukocyte-endothelial cell interactions." Febs J **273**(19): 4416-24.

Kataoka, N., K. Iwaki, et al. (2002). "Measurements of endothelial cell-to-cell and cell-to-substrate gaps and micromechanical properties of endothelial cells during monocyte adhesion." Proc Natl Acad Sci U S A **99**(24): 15638-43.

Katoh, K., Y. Kano, et al. (1998). "Isolation and contraction of the stress fiber." Mol Biol Cell **9**(7): 1919-38.

Keller, R., L. A. Davidson, et al. (2003). "How we are shaped: the biomechanics of gastrulation." Differentiation **71**(3): 171-205.

Ko, K. S., P. D. Arora, et al. (2001). "Cadherins mediate intercellular mechanical signaling in fibroblasts by activation of stretch-sensitive calcium-permeable channels." J Biol Chem **276**(38): 35967-77.

Lambert, M., O. Thoumine, et al. (2007). "Nucleation and growth of cadherin adhesions." Exp Cell Res **313**(19): 4025-40.

Leckband, D. and A. Prakasam (2006). "Mechanism and dynamics of cadherin adhesion." Annu Rev Biomed Eng **8**: 259-87.

Lemmon, C. A., N. J. Sniadecki, et al. (2005). "Shear force at the cell-matrix interface: enhanced analysis for microfabricated post array detectors." Mech Chem Biosyst **2**(1): 1-16.

Martin, A. C., M. Kaschube, et al. (2009). "Pulsed contractions of an actin-myosin network drive apical constriction." Nature **457**(7228): 495-9.

Maslin, C. L., K. Kedzierska, et al. (2005). "Transendothelial migration of monocytes: the underlying molecular mechanisms and consequences of HIV-1 infection." Curr HIV Res **3**(4): 303-17.

McVerry, B. J. and J. G. Garcia (2004). "Endothelial cell barrier regulation by sphingosine 1-phosphate." J Cell Biochem **92**(6): 1075-85.

Mehta, D., M. Konstantoulaki, et al. (2005). "Sphingosine 1-phosphate-induced mobilization of intracellular Ca2+ mediates rac activation and adherens junction assembly in endothelial cells." J Biol Chem **280**(17): 17320-8.

Millan, J. and A. J. Ridley (2005). "Rho GTPases and leucocyte-induced endothelial

remodelling." Biochem J **385**(Pt 2): 329-37.

Miyake, Y., N. Inoue, et al. (2006). "Actomyosin tension is required for correct recruitment of adherens junction components and zonula occludens formation." Exp Cell Res **312**(9): 1637-50.

Navarro, P., L. Caveda, et al. (1995). "Catenin-dependent and -independent functions of vascular endothelial cadherin." J Biol Chem **270**(52): 30965-72.

Nelson, C. M., R. P. Jean, et al. (2005). "Emergent patterns of growth controlled by multicellular form and mechanics." Proc Natl Acad Sci U S A **102**(33): 11594-9.

Nelson, C. M., D. M. Pirone, et al. (2004). "Vascular endothelial-cadherin regulates cytoskeletal tension, cell spreading, and focal adhesions by stimulating RhoA." Mol Biol Cell **15**(6): 2943-53.

Osborn, L., C. Hession, et al. (1989). "Direct expression cloning of vascular cell adhesion molecule 1, a cytokine-induced endothelial protein that binds to lymphocytes." Cell **59**(6): 1203-11.

Panes, J., M. Perry, et al. (1999). "Leukocyte-endothelial cell adhesion: avenues for therapeutic intervention." Br J Pharmacol **126**(3): 537-50.

Panorchan, P., M. S. Thompson, et al. (2006). "Single-molecule analysis of cadherin-mediated cell-cell adhesion." J Cell Sci **119**(Pt 1): 66-74.

Perez, T. D., M. Tamada, et al. (2008). "Immediate-early signaling induced by E-cadherin engagement and adhesion." J Biol Chem **283**(8): 5014-22.

Perret, E., A. Leung, et al. (2004). "Trans-bonded pairs of E-cadherin exhibit a

remarkable hierarchy of mechanical strengths." Proc Natl Acad Sci U S A **101**(47): 16472-7.

Petri, B. and M. G. Bixel (2006). "Molecular events during leukocyte diapedesis." Febs J **273**(19): 4399-407.

Pokutta, S. and W. I. Weis (2002). "The cytoplasmic face of cell contact sites." Curr Opin Struct Biol **12**(2): 255-62.

Pollard, T. D. and G. G. Borisy (2003). "Cellular motility driven by assembly and disassembly of actin filaments." Cell **112**(4): 453-65.

Potard, U. S., J. P. Butler, et al. (1997). "Cytoskeletal mechanics in confluent epithelial cells probed through integrins and E-cadherins." Am J Physiol **272**(5 Pt 1): C1654-63.

Rabodzey, A., P. Alcaide, et al. (2008). "Mechanical forces induced by the transendothelial migration of human neutrophils." Biophys J **95**(3): 1428-38.

Rao, R. M., L. Yang, et al. (2007). "Endothelial-dependent mechanisms of leukocyte recruitment to the vascular wall." Circ Res **101**(3): 234-47.

Rauzi, M., P. Verant, et al. (2008). "Nature and anisotropy of cortical forces orienting Drosophila tissue morphogenesis." Nat Cell Biol **10**(12): 1401-10.

Rayment, I., H. M. Holden, et al. (1993). "Structure of the actin-myosin complex and its implications for muscle contraction." Science **261**(5117): 58-65.

Rolo, A., P. Skoglund, et al. (2009). "Morphogenetic movements driving neural tube closure in Xenopus require myosin IIB." Dev Biol **327**(2): 327-38.

Scott, I. C. and D. Y. Stainier (2003). "Developmental biology: twisting the body into shape." Nature **425**(6957): 461-3.

Shaw, S. K., P. S. Bamba, et al. (2001). "Real-time imaging of vascular endothelial-cadherin during leukocyte transmigration across endothelium." J Immunol **167**(4): 2323-30.

Shewan, A. M., M. Maddugoda, et al. (2005). "Myosin 2 is a key Rho kinase target necessary for the local concentration of E-cadherin at cell-cell contacts." Mol Biol Cell **16**(10): 4531-42.

Shikata, Y., K. G. Birukov, et al. (2003). "S1P induces FA remodeling in human pulmonary endothelial cells: role of Rac, GIT1, FAK, and paxillin." J Appl Physiol **94**(3): 1193-203.

Skoglund, P., A. Rolo, et al. (2008). "Convergence and extension at gastrulation require a myosin IIB-dependent cortical actin network." Development **135**(14): 2435-44.

Somlyo, A. P. and A. V. Somlyo (2003). "Ca2+ sensitivity of smooth muscle and nonmuscle myosin II: modulated by G proteins, kinases, and myosin phosphatase." Physiol Rev **83**(4): 1325-58.

Springer, T. A. (1994). "Traffic signals for lymphocyte recirculation and leukocyte emigration: the multistep paradigm." Cell **76**(2): 301-14.

Steinberg, M. S. (1970). "Does differential adhesion govern self-assembly processes in histogenesis? Equilibrium configurations and the emergence of a hierarchy among populations of embryonic cells." J Exp Zool **173**(4): 395-433.

Takaishi, K., T. Sasaki, et al. (1997). "Regulation of cell-cell adhesion by rac and rho small G proteins in MDCK cells." J Cell Biol **139**(4): 1047-59.

Tan, J. L., J. Tien, et al. (2003). "Cells lying on a bed of microneedles: an approach to isolate mechanical force." Proc Natl Acad Sci U S A **100**(4): 1484-9.

Thompson, P. W., A. M. Randi, et al. (2002). "Intercellular adhesion molecule (ICAM)-1, but not ICAM-2, activates RhoA and stimulates c-fos and rhoA transcription in endothelial cells." J Immunol **169**(2): 1007-13.

van Buul, J. D., M. J. Allingham, et al. (2007). "RhoG regulates endothelial apical cup assembly downstream from ICAM1 engagement and is involved in leukocyte trans-endothelial migration." J Cell Biol **178**(7): 1279-93.

van Buul, J. D. and P. L. Hordijk (2004). "Signaling in leukocyte transendothelial migration." Arterioscler Thromb Vasc Biol **24**(5): 824-33.

van Nieuw Amerongen, G. P., R. Draijer, et al. (1998). "Transient and prolonged increase in endothelial permeability induced by histamine and thrombin: role of protein kinases, calcium, and RhoA." Circ Res **83**(11): 1115-23.

van Nieuw Amerongen, G. P., S. van Delft, et al. (2000). "Activation of RhoA by thrombin in endothelial hyperpermeability: role of Rho kinase and protein tyrosine kinases." Circ Res **87**(4): 335-40.

van Wetering, S., N. van den Berk, et al. (2003). "VCAM-1-mediated Rac signaling controls endothelial cell-cell contacts and leukocyte transmigration." Am J Physiol Cell Physiol **285**(2): C343-52.

Vasioukhin, V., C. Bauer, et al. (2000). "Directed actin polymerization is the driving force for epithelial cell-cell adhesion." Cell **100**(2): 209-19.

Vestweber, D. (2007). "Adhesion and signaling molecules controlling the transmigration of leukocytes through endothelium." Immunol Rev **218**: 178-96.

Vicente-Manzanares, M., X. Ma, et al. (2009). "Non-muscle myosin II takes centre stage in cell adhesion and migration." Nat Rev Mol Cell Biol **10**(11): 778-90.

Warren H. Lewis (1947). "Mechanics of invagination." The Anatomical Record **97**(2): 139-156.

Wojciak-Stothard, B. and A. J. Ridley (2002). "Rho GTPases and the regulation of endothelial permeability." Vascul Pharmacol **39**(4-5): 187-99.

Wojciak-Stothard, B., L. Williams, et al. (1999). "Monocyte adhesion and spreading on human endothelial cells is dependent on Rho-regulated receptor clustering." J Cell Biol **145**(6): 1293-307.

Worthylake, R. A. and K. Burridge (2001). "Leukocyte transendothelial migration: orchestrating the underlying molecular machinery." Curr Opin Cell Biol **13**(5): 569-77.

Yamada, S. and W. J. Nelson (2007). "Localized zones of Rho and Rac activities drive initiation and expansion of epithelial cell-cell adhesion." J Cell Biol **178**(3): 517-27.

Yamada, S., S. Pokutta, et al. (2005). "Deconstructing the cadherin-catenin-actin complex." Cell **123**(5): 889-901.

Yap, A. S., M. S. Crampton, et al. (2007). "Making and breaking contacts: the cellular biology of cadherin regulation." Curr Opin Cell Biol **19**(5): 508-14.